Since January 2020 Elsevier has created a COVID-19 resource centre with free information in English and Mandarin on the novel coronavirus COVID-19. The COVID-19 resource centre is hosted on Elsevier Connect, the company's public news and information website.

Towards Smart Diagnostic Methods for COVID-19: Review of Deep Learning for Medical Imaging

Marjan Jalali Moghaddam , Mina Ghavipour

PII: S2667-2588(22)00006-1
DOI: https://doi.org/10.1016/j.ipemt.2022.100008
Reference: IPEMT 100008

To appear in: *IPEM-Translation*

Received date: 1 February 2022
Revised date: 20 October 2022
Accepted date: 24 October 2022

Please cite this article as: Marjan Jalali Moghaddam , Mina Ghavipour , Towards Smart Diagnostic Methods for COVID-19: Review of Deep Learning for Medical Imaging, *IPEM-Translation* (2022), doi: https://doi.org/10.1016/j.ipemt.2022.100008

Towards Smart Diagnostic Methods for COVID-19: Review of Deep Learning for Medical Imaging

Marjan Jalali Moghaddam[1], Mina Ghavipour[2]*

[1,2] Department of Computer Engineering and Information Technology, Amirkabir University of Technology, Tehran, Iran

***Corresponding Author:**
Mina_ghavipour@aut.ac.ir
ORCID: 0000-0002-5222-2532

Highlights:

- We review DL techniques for diagnostics of COVID-19 based on CT and X-ray images
- We focus on peer-reviewed articles published in the period Jan 2020 to Oct 2021
- A comprehensive summary of the technical details of developed models is provided
- The challenges in the smart diagnosis of COVID-19 using DL are discussed
- Some recommendations are given for developing models with higher quality

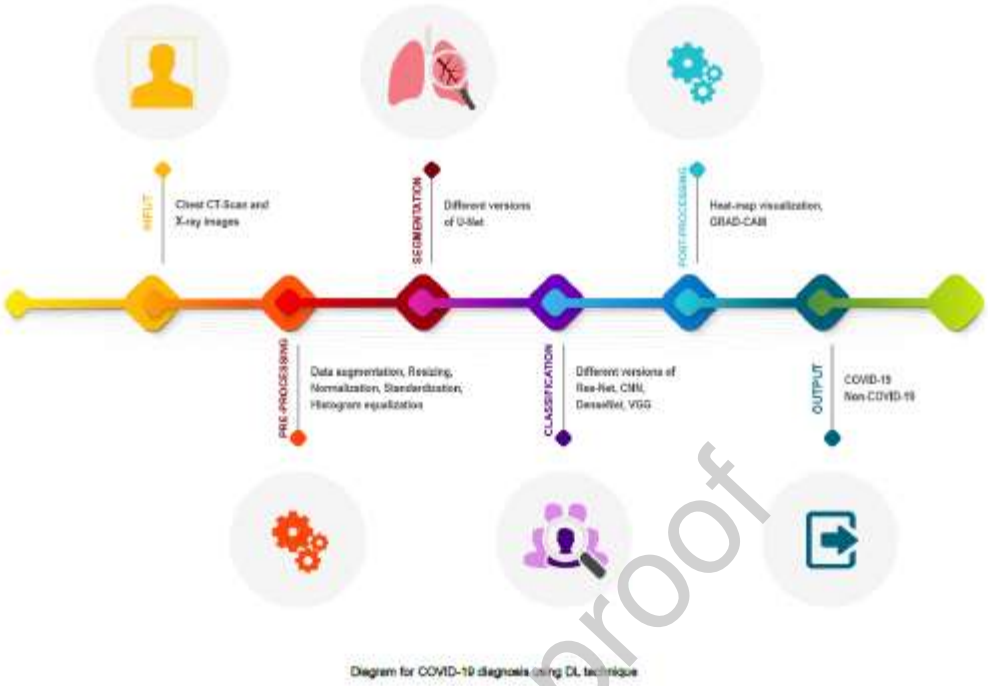

Diagram for COVID-19 diagnosis using DL technique

Abstract

The infectious disease known as COVID-19 has spread dramatically all over the world since December 2019. The fast diagnosis and isolation of infected patients are key factors in slowing down the spread of this virus and better management of the pandemic. Although the CT and X-ray modalities are commonly used for the diagnosis of COVID-19, identifying COVID-19 patients from medical images is a time-consuming and error-prone task. Artificial intelligence has shown to have great potential to speed up and optimize the prognosis and diagnosis process of COVID-19. Herein, we review publications on the application of deep learning (DL) techniques for diagnostics of patients with COVID-19 using CT and X-ray chest images for a period from January 2020 to October 2021. Our review focuses solely on peer-reviewed, well-documented articles. It provides a comprehensive summary of the technical details of models developed in these articles and discusses the challenges in the smart diagnosis of COVID-19 using DL techniques. Based on these challenges, it seems that the effectiveness of the developed models in clinical use needs to be further investigated. This review provides some recommendations to help researchers develop more accurate prediction models.

***Keywords**: Artificial Intelligence, Classification, Segmentation, CT-Scan, X-ray*

List of Abbreviations

ABBREVIATION	DEFINITION
Acc	Accuracy
AUC	the Area Under the ROC Curve
CNN	Convolutional neural network
COVID-19	Coronavirus disease 2019
CT	Computed Tomography
DL	Deep Learning
GAN	Generative Adversarial Network
GRAD-CAM	Gradient-weighted Class Activation Mapping
HIS	Hyperspectral Imaging
LRN	Local Response Normalization
LUS	Lung Ultrasound
PET	Positron Emission Tomography
Pre	Precision
ResNet	Residual Network
ROI	Region of Interest
RT–PCR	Reverse Transcriptase-Polymerase Chain Reaction
SARS-CoV-2	Severe Acute Respiratory Syndrome Coronavirus 2
SEM	Scanning Electron Microscopy
Sen	Sensitivity
Spe	Specificity
SVM	Support Vector Machine
Te	Test
Tr	Training
V	Validation
WHO	World Health Organization

Highlights

- We survey different DL techniques developed in the literature for the smart diagnosis of COVID-19 based on CT and X-ray chest images.
- We search for relevant studies published in the period from January 2020 to October 2021. Compared to other review articles, we cover a longer period for literature review.

- We only focus on peer-reviewed, well-documented articles. This way, our review provides researchers with informative works in this domain.
- Our paper provides a comprehensive summary of the technical details of DL models developed in reviewed articles. Therefore, researchers will be able to compare developed DL models, determine the best model settings, and find the main challenges.
- The challenges in the smart diagnosis of COVID-19 using DL models are discussed and some recommendations are given for alleviating challenges and developing models with higher quality.

1. Introduction

In early December 2019, the first case of COVID-19, the disease caused by the virus Severe Acute Respiratory Syndrome Coronavirus 2 (SARS-CoV-2), was confirmed by the authorities in Wuhan, China. COVID-19 developed rapidly into a global outbreak and spread all across the world. The World Health Organization (WHO) described the outbreak as a Public Health Emergency of International Concern on 30 January 2020 and declared it a pandemic on 11 March 2020. Globally, as of 6:06pm CEST, 19 October 2022, there have been 623,000,396 confirmed cases of COVID-19, including 6,550,033 deaths, reported to WHO (https://covid19.who.int).

Although Reverse Transcriptase-Polymerase Chain Reaction (RT–PCR) is the gold standard for diagnosing COVID-19 [1], the sensitivity of the test is relatively poor, and thus even in patients with a negative RT–PCR result, COVID-19 infection cannot be entirely excluded [2,3]. Therefore, medical imaging, especially chest computed tomography (CT) scan and X-ray, is often used to complement the RT–PCR test to achieve more diagnostic certainty. These imaging techniques have a higher sensitivity than RT–PCR and play a critical role not only in the early diagnosis and treatment of COVID-19 patients but also in monitoring the progress of the disease [2,3]. However, the accuracy of COVID-19 diagnosis using CT and X-ray chest images depends on radiological expertise, and some radiologists may fail to interpret accurately the results of these images, hence leading to reduced sensitivity [4,5].

With recent advances in machine learning techniques, particularly deep learning (DL), and the success of these techniques in medical image processing, scientists and clinicians hope to improve the accuracy of COVID-19 diagnosis by applying deep learning methods to chest medical images. These methods have the potential in providing decision support for clinicians and reducing medical errors. In a

short period, we have witnessed a large number of DL models developed for a very broad range of COVID-19-related applications. The purpose of the present review is to give more insight into deep learning applications in the diagnostics of COVID-19. We survey the literature on diagnosing patients infected by COVID-19 using DL techniques for a period from January 2020 to October 2021. Herein, our main focus is on classification and segmentation models proposed based on CT and X-ray chest images. Our review only includes peer-reviewed, well-documented articles and summarizes the technical details of models developed in these articles. We also discuss the challenges of using deep learning for the smart diagnosis of COVID-19. The challenges show that the performance of the models developed in the reviewed articles is probably optimistic and these models are not of potential for clinical use. We finally provide some recommendations that can help researchers develop more accurate and practical models for the COVID-19 diagnosis.

2. Methods

2.1. Data Sources and Search Strategy

This search was intended to address the question: “What deep learning techniques have been developed for the COVID-19 diagnosis using CT and X-ray images?”. For a period from January 2020 to October 2021, we conducted systematic searches of the following on-line databases in order to identify relevant works: IEEE Xplore, ScienceDirect, Springer, PubMed, and Google Scholar.

2.2. Search terms

The keywords used for the literature search were “COVID-19; Coronavirus; Diagnosis; Detection; Artificial Intelligence; Machine Learning; Deep Learning; Medical Imaging; CT-Scan; X-ray.’’ They were connected using “and’’, or “or’’ to identify the articles that deal with the diagnosis of COVID-19 using DL techniques on medical images.

2.3. Selection criteria

The studies with the following criteria were included in the review: 1) Articles that employed machine learning or deep learning techniques for the COVID-19 diagnosis, 2) Articles that utilized techniques to analyze radiographic images (CT scan, and/or X-ray), 3) Articles that applied classification and segmentation models.

The following exclusion criteria were used to eliminate studies from consideration: 1) Articles that were not in the English language, 2) Articles that were not published in peer-reviewed journals, 3) Review Articles, 4) Articles that did not use ML/DL approaches for diagnosing COVID-19 based on medical images, 5) Articles that did not provide a clear explanation of the implemented model and its results.

3. Technical Background

This review paper aims to survey different DL models developed in the literature for the smart diagnosis of COVID-19 in people with suspected infection. We focus on classification and/or segmentation techniques using CT and X-ray chest images. For this purpose, this section briefly discusses various DL architectures applied in the reviewed articles.

3.1. Classification Models

In this section, the different deep neural networks for COVID-19 classification based on CT and X-ray chest images are discussed.

Standard CNN. The architecture of convolutional neural networks (CNN) is inspired by human and animal brains. The main advantage of CNN is detecting relevant features automatically and without any human supervision. CNN tries to overcome the overfitting problem by using convolutional layers. Figure 1 depicts the architecture of standard deep CNN. The different parts of this architecture are described below:

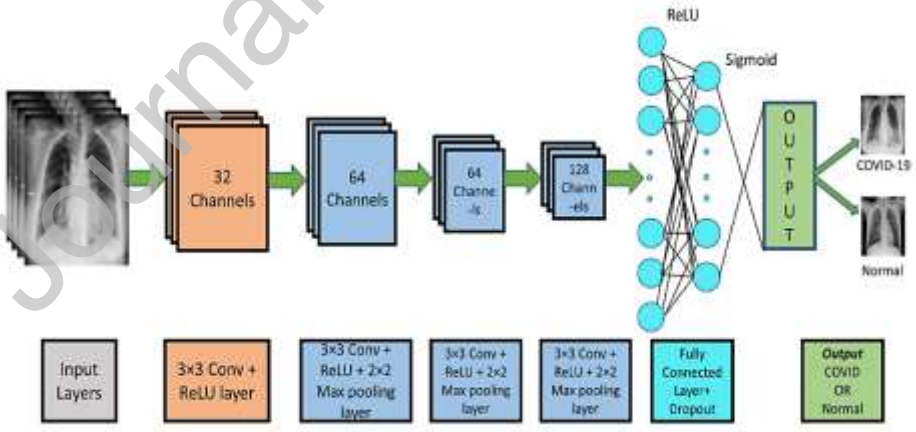

Fig. 1. A CNN model for COVID-19 Detection [6]

- The convolutional layer is the main building block of a CNN and applies a convolution operation to the input.
- The pooling layer reduces the dimensions of the feature maps.
- The fully connected layer is usually placed at the end of CNN architecture to do the classification task.

- The loss function calculates the prediction error. Through network learning, this value is optimized.
- Various techniques such as dropout, batch normalization, and data augmentation that are applied for better learning.

AlexNet. AlexNet is one of the earliest and most widely cited deep neural networks and a leading architecture for any object-detection task. It first introduced two new concepts named Local Response Normalization (LRN) and dropout to help the deep neural network learn better [7]. As a normalization layer, LRN implements the idea of lateral inhibition. Dropout is one of the regularization approaches to avoid the overfitting problem. It randomly skips some neurons during training and forces the other neurons in the layer to pick up the slack. The architecture of AlexNet is shown in Figure 2.

SqueezeNet. SqueezeNet is a convolutional neural network that utilizes design strategies to reduce the number of weights and is considered a more compact replacement for AlexNet [9]. On the ImageNet dataset, it achieves accuracies comparable to AlexNet while performing 3x faster and containing up to 50x fewer parameters. ImageNet (http://www.image-net.org) is a large-scale hierarchical dataset of annotated images for computer vision and machine learning research [10]. Figure 3 depicts a combined architecture of AlexNet, SqueezeNet, GoogleNet, and MobileNetV2.

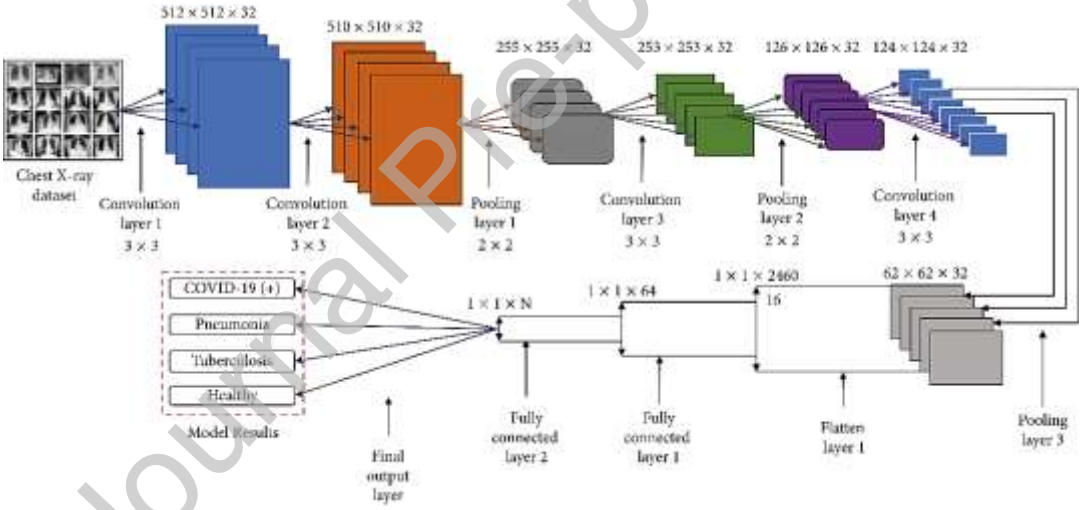

Fig. 2. AlexNet Architecture used for COVID-19 classification [8]

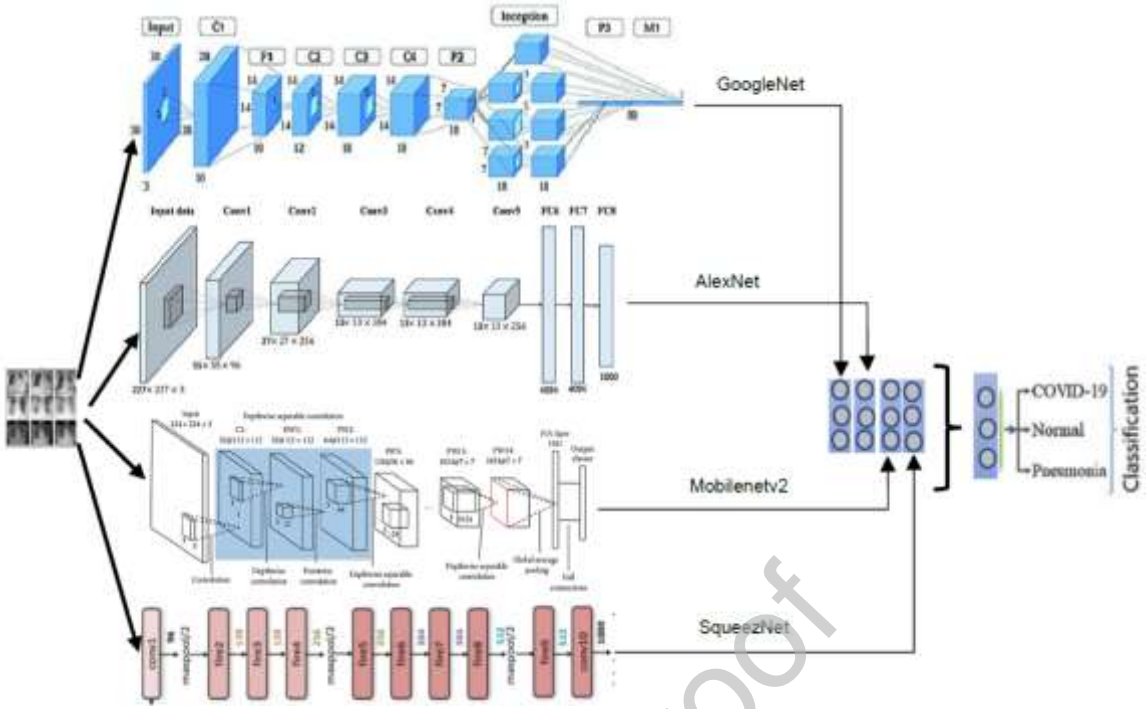

Fig. 3. A combined architecture of AlexNet, SqueezeNet, GoogleNet, and MobileNetV2 for *COVID-19* detection [12]

VGGNet. VGG is a classical CNN architecture. It consists of a few convolutional layers that apply the RELU activation function [11]. The number of convolution layers differs in various versions of VGG. A single max-pooling layer and three fully connected layers are placed following these activation layers, As shown in Figure 4. This architecture uses the Softmax classifier.

GoogleNet. GoogleNet, also called InceptionNet-V1, proposed the novel Inception blocks that improve recognition accuracy. The distinctive features of this architecture (see Figure 3) are the large convolution masks, the less dimensional space, and reduced computational complexity. GoogleNet is deeper with much fewer parameters compared to its ancestors AlexNet and VGG [11].

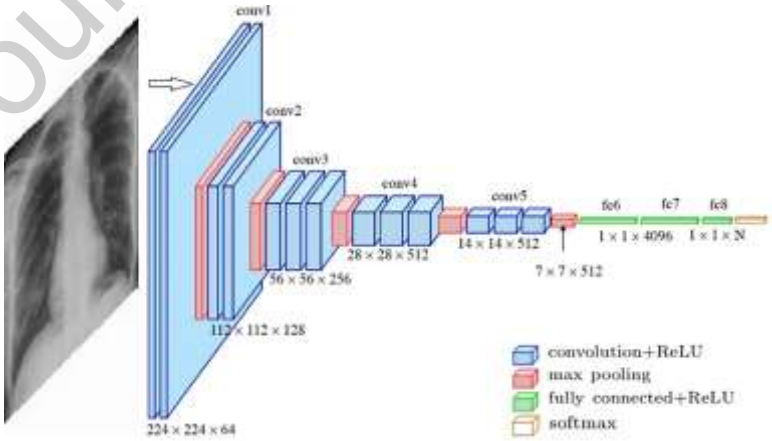

Fig. 4. The structure of VGG16 for COVID-19 detection [13]

MobileNet. The main characteristic of MobileNet (see Figure 3) is using depth-wise separable convolution that consists of two layers named depth-wise convolution and point-wise convolution. Using these layers, MobileNet provides an intensive reduction in model size and decreases computational

cost by about 8-9 times compared to standard convolutions. A RELU and batch normalization are placed after both of these layers. MobileNet is simple but efficient for mobile and embedded machine vision applications [14].

DenseNet. As a type of convolutional neural network, DenseNet utilizes dense connections between convolutional layers where each layer is connected to every other layer. DenseNet was introduced to overcome the issue of vanishing gradient. With effective usage of feature reuse, the network parameters decrease dramatically [15]. Figure 5 depicts the architecture of a DenseNet network.

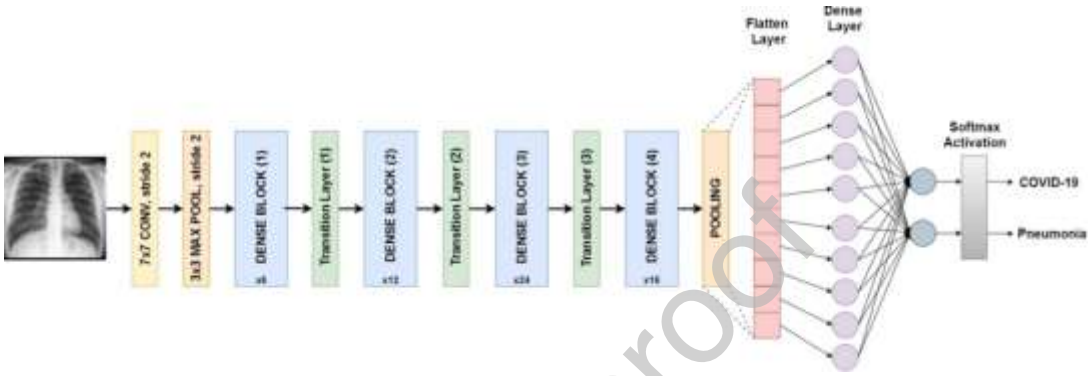

Fig. 5. DenseNet architecture designed for *COVID-19* classification [16]

ResNet. The core idea of the Residual network (ResNet) is introducing a technique called skip connection (or Shortcut Connection) that skips some of the layers in the network and feeds the output of a layer as the input to later layers, as shown in Figure 6. There are different variants of ResNet architecture composed of a different number of layers. The most popular type of ResNet network is ResNet50 including 49 convolutional layers followed by one fully connected layer [17].

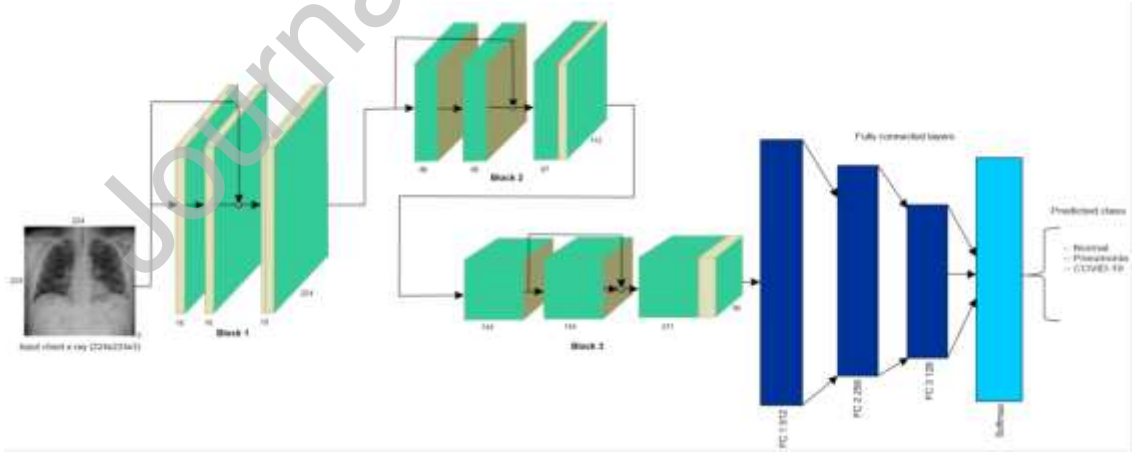

Fig. 6. ResNet architecture for COVID-19 image classification [18]

EfficientNet. The EfficientNet network relies on a compound scaling method that uniformly scales all three dimensions of depth/width/resolution while maintaining a balance between all network dimensions. using the compound scaling technique, the authors scaled the baseline network EfficientNet-B0 to get different variations including EfficientNet-B1 to B7. In comparison to squeeze-

and-excitation networks, EfficientNet is 7.7 x smaller and 10 x faster [19]. Figure 7 describes the architecture of an EfficientNet model proposed for COVID-19 image classification.

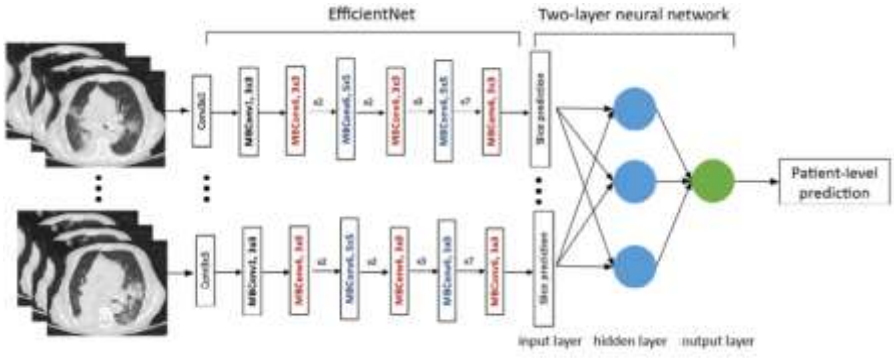

Fig. 7. EfficientNet model for COVID-19 classification [20]

InceptionNet. An inception network is composed of repeating components referred to as Inception modules. InceptionNet employs the idea of auxiliary classifiers to address the gradient vanishing problem and improve the convergence of very deep networks. It also applies different convolution kernels of various sizes in parallel. This architecture helps to extract similar features in different sizes simultaneously. The popular versions of InceptionNet are InceptionV1 to V3 (as shown in Figure 8) and Inception-ResNet.

3.2. Segmentation Models

The most common deep learning model developed for image segmentation, U-Net, has been widely utilized for lung region segmentation to diagnose COVID-19 patients:

U-NET. U-Net architecture is primarily designed for segmentation applications. Its good performance in segmenting medical images makes it the primary tool for segmentation in this field. The U-Net architecture is an almost symmetrical u-shape network that consists of two paths called decoder and encoder. It is much faster than other segmentation networks, because of its context-based learning [21]. The architecture of U-Net is described in Figure 9.

Fig. 8. InceptionV3 architecture for *COVID-19* classification [16]

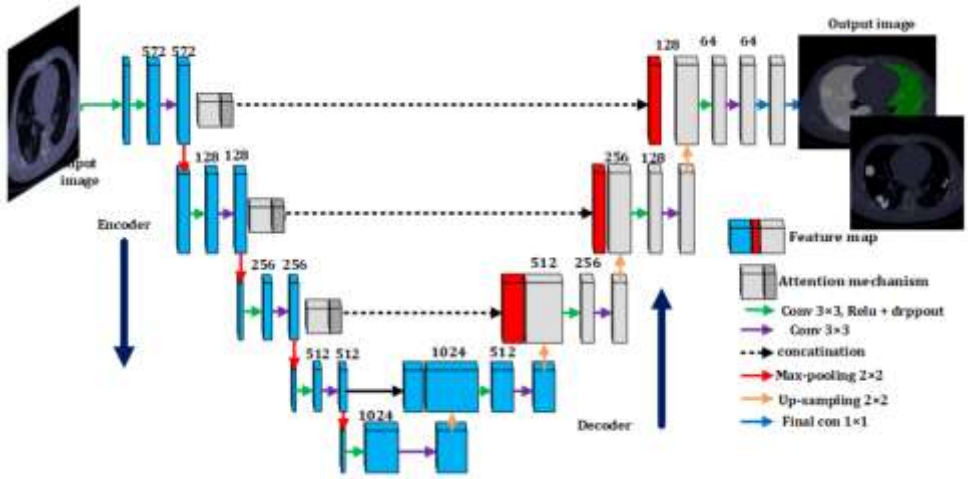

Fig. 9. The architecture of U-Net for COVID-19 segmentation [22]

3.3. Generative Adversarial Networks

Generative Adversarial Network (GAN) is an unsupervised approach and a powerful method to produce unseen data samples with the same statistics as the training set. This way, it can overcome overfitting and data shortage problems and improve deep network performance. GAN architecture (as shown in Figure 10) is composed of two sub-models named generator model and discriminator model contesting each other in a game. The generator model tries to generate new plausible images similar to real data. The discriminator model tries to distinguish between real and fake samples. This process continues until the generator samples become close to the actual input samples [11].

4. Results

From all the databases considered for finding relevant works (see Section 2.1 for more information), we identified 15,417 articles that satisfied our search terms, of which, 6209 articles were preprints (not peer-reviewed) and excluded from this review. For duplicate studies (157 articles), we ensured that the latest version of the article was considered. The titles, abstracts, and full texts were screened for relevance and eligibility. We removed 8983 articles that were irrelevant or not documented with enough detail to allow other researchers to reliably reproduce the results. Finally, our investigation retained 68 peer-reviewed, well-documented articles for consideration in this review. This section presents all the technical details of DL models developed in these articles for COVID-19 diagnosis in summary and explains the advantages and disadvantages of the used techniques. Table 1 summarizes the reviewed articles and reports informative details for them.

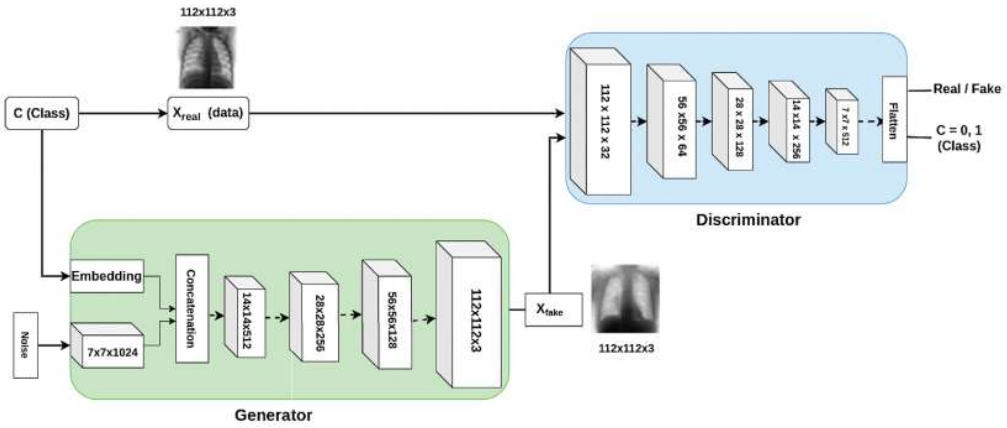

Fig. 10. A GAN architecture for *COVID-19* detection [23]

Generally, imaging modalities considered in COVID-19 diagnosis are X-ray, Computed Tomography (CT), and ultrasound. Although ultrasound imaging is a more widely available, cost-effective, safe, and real-time imaging technique [24], it has a relatively lower sensitivity in comparison to chest CT-Scan [25] and cannot usually detect lesions that are deep and intrapulmonary [26,27]. Since more deep learning-based COVID-19 detection and segmentation works focus on CT and X-ray modalities, we only reviewed articles that have used these modalities. The column *Imaging Modality* in the table indicates which imaging modalities have been used as the input to the DL network developed in each article. Chest radiological imaging, such as CT and X-ray, has a vital role in the early diagnosis and treatment of COVID-19 disease [28].

The second column *Dataset* refers to image datasets collected by or utilized in the reviewed articles. These datasets contain CT and/or X-ray images from healthy, COVID-19, and Non-COVID patients. Since COVID-19 is a new disease, there is no dataset of appropriate size for its diagnosis purpose. Therefore, many works combine images from several different publicly available datasets, gather chest images from multiple institutions, or use a combination of their clinical images and public datasets.

The column # *Cases Per Class* indicates the number of images/patients in each class. In other words, the value of each cell in this column shows which classes have been considered in the corresponding article, and how many images or patients there are in each class. COVID-19 datasets are strongly imbalanced which can impact the model accuracy. Hence, several studies have proposed different class balancing techniques to overcome the data imbalance issue [29].

The column *Test Method* shows which technique has been used for splitting data into three non-overlapping parts including the Training (Tr) set, Validation (V) set, and Test (Te) set. The division of input data into these three subsets is crucial in the creation of robust prediction models to avoid overfitting, as well as to increase generalization. Overfitting is one of the main issues in the training of machine learning algorithms [30]. It occurs when the training error is low, and the generalization error is

high. Although a small training dataset is the main reason for the overfitting problem, the complexity of the model can be another reason [31]. Many works apply a validation set to identify the overfitting problem during the model training by controlling the model complexity [32]. It can help the model determine when to stop the training process. For simplicity, we use two different patterns for reporting the test method. The first pattern is Tr%: V%: Te% which indicates the percent of data assigned to each part, and the second pattern is Tr-V-Te showing the number of data assigned to each part. We use the phrase “Separate DB” for indicating the studies which have utilized separate datasets for training and testing their DL models.

The column *Validation Method* refers to the validation method used to evaluate the efficiency of DL models. The applied validation methods contain K-fold cross-validation and the holdout method. The K-fold cross-validation technique ensures that every observation from the original dataset has the chance of appearing in the training and test sets [33]. In this approach, at first, the data is randomly split into K equal-sized folds (the K value is usually selected in the range of five to ten depending on the data size). Then, the model is trained on the K-1 folds and validated on the remaining fold. This process is repeated K times, with each of the K folds used exactly once as the test set. This technique is one of the best validation approaches if there are not enough instances to train on [34]. On the other hand, the holdout method partitions data randomly into two sets, training, and test. The size of the test set is typically smaller than that of the training set. Since the method involves a single run, results depend on how the data is split into these two sets [35]. The holdout method is not effective for comparing multiple models and tuning their hyper-parameters. Therefore, another very popular form of this method is usually utilized which splits data into three separate sets including training, validation, and test sets [36]. The validation set which is a holdout subset from the training set is used to tune various hyper-parameters and choose the best performing model. The final model is evaluated by the test set and the found error is considered the generalization error.

The dataset used for the transfer learning process is reported in the column *Transfer Learning*. The philosophy behind transfer learning is that people can intelligently utilize knowledge learned in the past to solve new problems faster or more efficiently [37]. Transfer learning is an approach in machine learning where knowledge learned in one or more tasks is transferred to improve learning in another related task [38]. The main goal of this technique is to decrease training task time, improve generalization performance [39], and deal with small input dataset problems [40]. Transfer learning has

been widely adopted in many COVID-19 studies to compensate for the scarcity of large-scale public datasets for this disease.

The column *Learning Method* can contain the values Supervised, Unsupervised, Semi-supervised, and Weakly-supervised, showing which machine learning approach has been used for training the deep neural network. Supervised learning refers to a class of methods that learn on a labeled dataset, where each training sample is a pair of inputs and its desired output [41]. In an unsupervised learning model, in contrast, the algorithm tries to extract features and patterns from unlabeled data. In other words, the algorithm does not receive any feedback from the environment [42]. Clustering, association, and dimensionality reduction are three main tasks in unsupervised learning. A weakly-supervised model utilizes training data with incomplete, inexact, and inaccurate annotation [43]. Finally, semi-supervised learning describes a class of algorithms that seek to learn from both unlabeled and labeled samples typically assumed to be sampled from the same or similar distributions [44].

Since labeling lesion annotations is time-consuming and impractical for clinicians [45], Noisy labels exist widely for the segmentation of large-scale 3D medical images. It can be either due to challenges for accurate annotation, such as low contrast, ambiguous boundaries, and complex appearances of the target, or caused by low-cost inaccurate annotations such as annotations provided by non-experts, human-in-the-loop strategies [46], and some algorithms generating pseudo labels [47,48]. For this reason, some COVID-19 studies have applied weakly supervised or semi-supervised learning frameworks in their segmentation tasks.

The pre-processing functions applied to input images are shown in the column *Pre-processing*. In image processing, the pre-processing phase aims to process raw input images to improve the quality of images, produce a more understandable format for the algorithm, enhance accuracy, increase the number of data, reduce the processing time, or standardize data acquired from multiple devices [49,50]. There are several important steps in the pre-processing phase, such as data augmentation, histogram equalization, image normalization, morphological operators, segmentation, standardization, etc.

The column *Classification* categorizes COVID-19 classification models into two main groups: COVID-19 from Non-COVID and COVID-19 from Other Pneumonia. The former indicates a two-class classification where the class Non-COVID includes common pneumonia cases and non-pneumonia cases, and the latter shows a multi-class classification that distinguishes among COVID-19, other types of pneumonia, and healthy cases.

The column *Segmentation* classifies COVID-19 segmentation models into two categories. The first category, called the Lung-Region-Oriented method [49,51,52], is a prerequisite step in COVID-19 applications and separates the whole lung region and lung lobes from other regions in input images. The second category, called the Lung-Lesion-Oriented method [46,53], aims to separate lesions or metal and motion artifacts from the lung regions which is a challenging detection task.

The column *DNN*, which stands for deep neural network, shows the networks utilized for classification and segmentation tasks. In addition to well-known models, some new DNNs have been also introduced in the reviewed articles to detect COVID-19 infection in CT and X-ray chest images.

The value of the column *Classifier* indicates the classifier algorithm used in deep learning models for COVID-19 diagnosis purposes. These functions are applied in the last layer of a neural network. Some of the most used classifiers are introduced as follows. The Softmax function [54] normalizes the real values of the input vector into a probability distribution consisting of probabilities. The output values are in the interval (0,1). The support vector machine (SVM) [55] constructs a set of hyperplanes that provide the maximum margin distance to generate the least generalization error. The Sigmoid function [54], also called the logistic function, is a very popular activation function for artificial neural networks. The input value to this function is transformed into a probability that is between 0 and 1. The Majority Voting classifier [56] merges different classification rules to produce a classifier that is superior to any of the individual ones. It classifies each input value in the class that obtains a large number of votes.

The column *Post-processing* shows post-processing procedures applied to the output of a deep neural network. Some of the most common post-processing techniques include generating heat-map, heat-map visualization, calculating infection confidence, and GRAD-CAM (Gradient-weighted Class Activation Mapping).

Finally, the column *Performance Criteria* reports the performance of deep learning models developed in the studies. The common performance criteria contain Accuracy (Acc), Sensitivity (Sen), Specificity (Spe), F1-score, Precision (Pre), Recall, and the area under the ROC curve (AUC).

It is worth mentioning that some of the reviewed articles have proposed several DL models for COVID-19 diagnosis purposes or evaluated their models in two-class and multi-class modes. In these cases, for each study, we only provide the details of the model which has obtained the best result that may be the most helpful to researchers.

5. Discussion

During the recent coronavirus pandemic, RT-PCR frequently produced false-negative findings that increased over time [57]. Due to high false-negative rates, this test sometimes considers COVID-19 patients to be healthy people, which has severe consequences. The probability of a false-negative result on one day a patient has contracted the virus is 100% and falls to 67% over the four days of infection. On day five, the typical time of symptom onset, the chance of a false-negative result is 38% and drops to 20% on day eight. Then it begins to increase again, from 21% on day nine to 66% on day 21 [58]. As a result, an earlier diagnosis tool is necessary to reduce the spread of the disease.

Chest imaging could be a part of COVID-19 diagnosis in suspected or portable COVID-19 patients in the absence of an RT-PCR test, or where the RT-PCR test results are delayed or are negative in the early infection stage in the presence of symptoms indicative of COVID-19 [59]. Benmalek et al. [60] reported the typical imaging features for confirmed COVID-19 pneumonia cases which can help in the early screening and tracking of the disease.

The chest CT scan has been found to have a sensitivity value of 98% and is one of the most precise methods for diagnostics of this disease [61]. Hence, a chest CT may be viewed as a reliable complementary diagnostic measure for RT-PCR to help physicians assess patients more perfectly [20]. The report by Li et al. [62] showed that an initial CT scan performed as early as 5 days after the onset of symptoms would allow for a confident separation of severe and non-severe patients. Lung abnormalities on chest CT peak within 6–13 days after the initial onset of symptoms reaching the highest severity score [63–65]. On the other hand, X-ray has a reported sensitivity of 69% for COVID-19 diagnosis [66]. However, compared to CT, it is faster, less harmful, easy to perform, and costs less [67]. The radiographic findings detected on chest X-ray in COIVD-19 patients show the greatest severity on days 5–10 of symptom onset [68].

Table 1: Summary of recent DL techniques for COVID-19 diagnosis

Ref.	Modality	Dataset	# Cases per Class	Test Method	Validation Method	Transfer Learning	ML Approach	Preprocessing	Classification	Segmentation	DNN	Classifier	Postprocessing	Performance Criteria (%)
[69]	X-ray	Combination of Two Different DBs	142 COVID-19, 142 Normal Img.	70%:30%	Hold-out	ImageNet	Supervised	Resizing, Data Augmentation	COVID-19 from Non-COVID-19	NA	NCOVnet (Based on VGG-16)	Softmax	NA	Acc=97.62,Sen=97.62, Spe=78.57
[70]	X-ray	Combination of Two Different DBs	295 COVID-19, 65 Normal, 98 Pneumonia Img.	70%:30%	5-fold	NA	Supervised	Fuzzy Color Method, Image Stacking Technique	COVID-19 from Other Pneumonia	NA	MobileNetV2, SqueezeNet	SVM	Social Mimic Optimization Method	Acc=99.27
[71]	X-ray	Combination of Two Different DBs	105 COVID-19, 11 SARS, 80 Normal Img.	70%:30%	Hold-out	ImageNet	Supervised	Data Augmentation, Histogram, Feature Extraction using AlexNet, PCA, K-means	COVID-19 from Other Pneumonia	NA	DeTraC (Based on ResNet18), AlexNet (Feature Extraction)	Softmax	Composition Phase	Acc=95.12,Sen=97.91, Spe=91.87
[72]	X-ray	COVIDx	76 COVID-19, 1583 Normal, 4290 Pneumonia Img.	80%:10%:10%	Hold-out	NA	Supervised	Data Augmentation, RGB format, Normalizing	COVID-19 from Other Pneumonia	NA	COVIDiagnosis-Net (Based on Deep SqueezeNet with Bayes Optimization)	Decision-Making System	Class Activation Mapping Visualization (Heat Map)	Acc=98.3,Spe=99.13, F1-Score=98.3
[73]	X-ray	Combination of Two Different DBs	127 COVID-19, 500 No-Findings, 500 Pneumonia Img.	80%:20%	5- fold	NA	Supervised	NA	COVID-19 from Non-COVID-19	NA	DarkCovidNet (Based on CNN)	Linear	Heatmaps Visualization	Acc=98.08,Spe=95.3, Sen=95.13,Pre=98.03, F1-Score=96.51
[74]	X-ray	RYDLS-20	90 COVID-19, 10 MERS, 11 SARS, 10 Varicella, 12 Streptococcus, 11 Pneumocystis Img.	70%:30%	Hold-out	ImageNet	Supervised	Different Features, Early Fusion, Late Fusion, Different Resampling Algorithms	COVID-19 from Other Pneumonia	NA	Inception-V3	Clus-HMC Framework	Friedman Statistical Test for Ranking	F1-Score=88.89
[75]	X-ray	Combination of Two Different DBs	284 COVID-19, 310 Normal, 330 Pneumonia Bacterial, 327 Pneumonia Viral Img.	75%:25%	4-fold	ImageNet	Supervised	Rescaling	COVID-19 from Other Pneumonia	NA	CoroNet (Based on Xception Architecture)	Softmax	NA	Acc=89.5,Pre=97, F1-Score=98
[76]	X-ray	Combination of Four Different DBs	455 COVID-19, 2109 Non-COVID Img.	90%:10%	10-fold	NA	Supervised	Rescaling, Data Augmentation	COVID-19 from Non-COVID-19	NA	MobileNet V2	NA	NA	Acc=99.18,Sen=97.36, Spe=99.42
[23]	X-ray	Combination of Three Different DBs	403 COVID-19, 721 Non-COVID Img.	932-192	Hold-out	NA	Supervised	Resizing, Normalization, Data Augmentation using CovidGAN Based AC-GAN	COVID-19 from Non-COVID-19	NA	VGG16	Softmax	PCA Visualization	Acc=95,Sen=90, Spe=97
[77]	X-ray	Combination of Three Different DBs	69 COVID-19, 79 Normal, 79 Pneumonia Viruses, 79 Pneumonia Bacterial Img.	72%:18%:10%	Hold-out	ImageNet	Supervised	Data Augmentation using GAN	COVID-19 from Non-COVID-19	NA	GoogleNet	Softmax	NA	Acc=100,Pre=100,F1-Score=100
[78]	X-ray	Combination of Three Different DBs	224 COVID-19, 504 Healthy, 400 Bacteria, 314 Viral Pneumonia Img.	90%:10%	10-fold	ImageNet	Supervised	Resizing	COVID-19 from Non-COVID-19	NA	MobileNet	NA	NA	Acc=96.78,Sen=98.66, Spe=96.46
[49]	X-ray	Pediatric cxr,Twitter COVID-19 cxr, Montreal COVID-19 cxr DBs	7595 Normal, 6012 Pneumonia of Unknown Type, 2780 Bacterial, 313 COVID-19 Img.	72%:18%:10%	Hold-out	ImageNet	Supervised	Pixel Rescaling, Median Filtering for Noise Removal and Edge Preservation, Normalization, Standardization for Identical Feature Distribution	COVID-19 from Other Pneumonia	Lung Region-Oriented Method	U-Net (Segmentation), Ensemble of Pruned Models: VGG-16, VGG-19, and Inception-V3 (Classification)	Softmax	Grad-CAM	Acc=99.01,Sen=99.01, Pre=99.01,F1-Score=99.01, AUC=99.72,MCC=98.2
[79]	X-ray	Combination of Two Different DBs	180 COVID-19, 6054 Pneumonia, 8851 Normal Img.	3784-11302	5-fold	ImageNet	Supervised	Data Augmentation	COVID-19 from Other Pneumonia	NA	Concatenation of the Xception and ResNet50V2	Softmax	NA	Acc=91.4
[80]	X-ray	Combination of Two Different DBs	181 COVID-19, 364 Healthy Img.	80%:20%:20%	Hold-out	ImageNet	Supervised	Normalization, Resizing	COVID-19 from Non-COVID-19	NA	VGG-19	Softmax	NA	Acc=96.3
[39]	X-ray	Combination of Three Different DBs	250 COVID-19, 2753 Other Pulmonary Diseases, 3520 Healthy Img.	2000-803-1100	Hold-out	ImageNet	Supervised	Resizing, Data Augmentation	COVID-19 from Other Pneumonia	NA	VGG-16	Softmax	Grad-CAM	Acc=98,Sen=87, Spe=94,F1-Score=89
[53]	X-ray	Combination of three Clinical DBs	610 COVID-19, 1493 Non-COVID-19, 1888 Normal, 305 Pneumonia Viral, 3085 Bacterial Pneumonia Img.	80%:20%	5-fold	Clinical	Supervised	Reshaping to Different Resolutions, Normalization	COVID-19 from Non-COVID-19	NA	Stacked Multi-Resolution CovXNet	Stacking using Meta-Learner	Grad-CAM	Acc=97.4,Spe=94.7, F1-Score=97.1, Recall=97.8,Pre=96.3, AUC=96.9
[81]	X-ray	Combination of Different DB	162 COVID-19, 2003 Healthy, 4280 Viral and Bacterial Pneumonia, 400 Tuberculosis Img.	90%:10%	10-fold	ImageNet	Supervised	Resizing, Normalization, Data Augmentation using CovidGAN Based AC-GAN	COVID-19 from Other Pneumonia	NA	Truncated InceptionNet V3	Softmax	Activation Maps Generation	Acc=98.77,Sen=95, Spe=99,Pre=99, F1-Score=97
[82]	X-ray	Combination of Five Different DBs	180 COVID-19, 191 Normal, 54 Bacterial Pneumonia, 20 Viral Pneumonia Img.	70%:10%:20%	Hold-out	ImageNet	Supervised	Standard Preprocessing, Segmentation, Data Type Casting, Histogram Equalization, Gamma	COVID-19 from Other Pneumonia	Lung Region-Oriented Method	ResNet18 (Classification), FC-DenseNet103	Majority Voting	Probabilistic Grad-CAM Saliency Map Visualization	Sen=100,Pre=76.9

								Correction, Resizing			(segmentation)			
[83]	X-ray	COVIDx, Clinical DB	9466 Normal, 9501 Non-COVID Pneumonia, 283 COVID-19 Img.	90%:10%	10-fold	NA	Supervised	NA	COVID-19 from Non-COVID-19	NA	Faster R–CNN	NA	NA	Acc=97.36,F1-Score=98.46,Pre=99.29, Spe=95.48,Sen=97.65
[40]	X-ray	Combination of Two Different DBs	1428 COVID-19, 700 Bacterial Pneumonia, 504 Healthy Img.	70%:30%	Hold-out	ImageNet	Supervised	Data Augmentation	COVID-19 from Non-COVID-19	NA	VGG-16	Softmax	Grad-CAM	Acc=96
[84]	X-ray	Combination of Three Different DBs	585 Abnormal, 585 Normal Img.	1000-170	Hold-out	ImageNet	Supervised	Resizing, Data Augmentation	COVID-19 from Non-COVID-19	NA	ResNet18	Softmax	NA	Acc=98,Sen=99, Spe=97,Pre=97, AUC=98
[85]	X-ray	Combination of Three Different DBs	137 COVID-19, 150 Pneumonia Img.	80%:20%	5-fold	ImageNet	Supervised	Resizing, Data Augmentation, Normalization	COVID-19 from Other Pneumonia	NA	Inception V3	Softmax	Grad-CA, resize	AUC=1,Acc=100, Sen=99,Spe=100
[50]	X-ray	BIMCV-COVID19+, PadChest, Clinical DB	2589 COVID-19, 4337 Normal Img.	80%:20%	5-fold	NA	Supervised	Histogram Matching Process, Rib Shadows Suppression, Convert to Grayscale, Contrast Enhancement by Contrast Limited Adaptive Histogram Equalization, Data Augmentation, Random Rotations, Width and Height Shift, Shear, Zoom, Horizontal Flips	COVID-19 from Non-COVID-19	Lung Region-Oriented Method	U-Net (Segmentation), COVID-Xnet (Based on CNN, Classification)	Softmax	Grad-CAM	Acc=94.43,AUC=98.8, F1-score=93.14, Pre=93.76,Spe=96.3, Sen=92.53
[86]	X-ray	Combination of Four Different DBs	219 COVID-19, 1341 Normal, 1345 Viral Pneumonia Img.	70%:30%	Hold-out	NA	Supervised	Data Augmentation	COVID-19 from Other Pneumonia	NA	CNN	SVM	NA	Acc=98.97,Sen=89.39, Spe= 99.75,F1-Score=96.72
[6]	X-ray	Clinical	659 Normal, 295 COVID-19 Img.	80%:20%	Hold-out	NA	Supervised	NA	COVID-19 from Non-COVID-19	NA	CNN	Sigmoid	NA	Acc=97.5,F1-Score=97.5,Pre=97.5, Recall=97.5,ROC=0.975
[87]	X-ray	Combination of Two Different DBs	202 COVID-19, 300 Normal, 300 Pneumonia Img.	80%:20%	5-fold	ImageNet	Supervised	Intensity Normalization, Class-label Encoding, Data Augmentation by CycleGAN, Width and Height Shift, Random Rotation, Horizontal Flips	COVID-19 from Other Pneumonia	NA	EfficientNetB0	Softmax	Grad-CAM	Acc=96.8
[88]	X-ray	Combination of Two Different DBs	224 COVID-19, 700 Bacterial, 504 Healthy Patients	70%:30%	Hold-out	ImageNet	Supervised	Data Augmentation, Resizing	COVID-19 from Non-COVID-19	NA	VGG-16	Softmax	Grad-CAM (to highlight the regions of interest)	Acc=96,spec=97.27, Sen=92.64
[89]	X-ray	Combination of Different DBs	2665 COVID-19, 3692 Pneumonia, 3692 Normal	9149- 450- 450	NA	ImageNet	Supervised	Data Augmentation, Resizing, Lung Segmentation, CLAHE histogram equalization, Denoising	COVID-19 from Non-COVID-19	Lung Region-Oriented Method	VGG-19 (Classification), U-Net (Segmentation)	Naive Bayes	Grad-CAM visualization	Acc=98.67,Kappa score=0.98,F1-Score=100
[90]	X-ray	Cohen and Kaggle	455 Normal, 457 Bacterial Pneumonia, 470 Viral Pneumonia (Stage1), 480 Viral Pneumonia (Stage2), 440 COVID-19 Img.	80%:20%	5-fold	ImageNet	Supervised	Resizing, Normalization, Data Augmentation	COVID-19 from Other Pneumonia	NA	Resnet101	Softmax	Grad-CAM visualization	Acc=98.93,Sen=98.93, Spec=98.66,Pre=96.39, F1-score=98.15
[5]	X-ray	COVIDx	8066 Normal, 5521 Pneumonia, 183 COVID-19 Img.	13569-231	NA	ImageNet	Supervised	Intensity Normalization, Resizing, Data Augmentation	COVID-19 from Other Pneumonia	NA	EfficientNet	Swish	NA	Acc=93.9,Sen=96.8, PPV=100
[91]	X-ray	Kaggle	219 COVID-19, 1341 Normal, 1345 Viral Pneumonia Img.	70%:10%:20%	5-fold	NA	Supervised	Cropping, Resizing	COVID-19 from Other Pneumonia	NA	CVDNet	Softmax	NA	Acc=96.69
[92]	X-ray	Combination of Six Different DBs	900 COVID-19, 900 Normal, 900 Pneumonia Img.	70%:30%	Hold-out	ImageNet	Supervised	Resizing, Converting to Color Image	COVID-19 from Other Pneumonia	NA	E-DiCoNet	ELM	NA	Acc=94.07,Sen=98.15, Spec=91.48
[93]	X-ray	Combination of Three Different DBs	543 COVID_19, 600 Normal, 600 Pneumonia Img.	1220-523	Hold-out	ImageNet	Supervised	Resizing	COVID-19 from Other Pneumonia	NA	AlexNet, ReliefF	SVM	NA	Acc=98.64,Spec=98.64, Sen=98.64, F-score=98.63
[94]	X-ray	chest X-ray (CXR) dataset	27 Normal, 220 SARS, 17 Streptococcus Img.	80%:20%	5-fold	ImageNet	Supervised	Noise Removal by Wiener Filtering	COVID-19 from Other Pneumonia	NA	FM-CNN	MLP	NA	Acc=98.06,Spec=98.29, Sen=97.22, F-score=97.93
[95]	X-ray	Combination of Different DBs	423 COVID-19, 1341 Normal, 1345 Viral PNA Img.	80%:20%	5-fold	ImageNet	Supervised	Image Resize, CLAHE Image Enhancement, Image Augmentation	COVID-19 from Other Pneumonia	NA	VGG-19	LMPL (Large margin piecewise linear)	Heatmap Visualization	Acc=99.39,F1-score=99.45,Pre=99.47, Sen=99.42

[96]	CT-Scan	Clinical	219 COVID-19, 224 Other Pneumonia, 175 Healthy Img.	85.4% : 14.6%	Hold-out	NA	Supervised	Segmentation, Data Augmentation	COVID-19 from Other Pneumonia	Lung Region-Oriented Method	ResNet-18 (Classification), VNET-IR-RPN (Segmentation)	Voting Strategy	Total Infection Confidence Score Calculation using Probability Formula of the Noisy-or Bayesian Function	Acc=86.7,Pre=81.3,F1-Score=83.9
[97]	CT-Scan	COVID-19 DB	1262 Positive COVID-19, 1230 Negative COVID-19 Img.	68%:17%:15%	Hold-out	ImageNet	Supervised	Data Augmentation	COVID-19 from Non-COVID-19	NA	DenseNet201	Sigmoid	NA	Pre=96.29,Recall=96.29, F1-Score=96.29, Spe=96.21,Acc=96.25
[98]	CT-Scan	Clinical	368 COVID-19 Patients, 127 Patients with Other Pneumonia	395-50-50	Hold-out	NA	Supervised	Segmentation using Threshold Segmentation and Morphological Optimization Algorithms, Rescaling, Multi-view Fusion	COVID-19 from Other Pneumonia	Lung Region-Oriented Method	ResNet50	Dense Layer	NA	Acc=76,Sen=81.1, Spe=61.5
[99]	CT-Scan	Combination of Different DBs	1029 COVID-19, 1695 Non-COVID Img.	1059-328-1337	Hold-out	NA	Supervised	Clipping, Cropping, Data Augmentation by Image Intensity and Contrast Adjustment, Random Gaussian Noise, Flipping, and Rotation	COVID-19 from Non-COVID-19	Lung Region-Oriented Method	DensNet-121 (Classification), AH-Net (Segmentation, Based on ResNet50)	NA	Grad-CAM	Acc=90.8,Sen=84, Spe=93,ppv=79.4, npv=94.8,Auc=94.9
[100]	CT-Scan	Clinical	108 COVID-19, 86 Non-COVID Patients	80%:20%	Hold-out	ImageNet	Supervised	Different Methods	COVID-19 from Non-COVID-19	NA	ResNet-101, Xception	Softmax	NA	Sen=98.04,Spe=100, Acc=99.02
[101]	CT-Scan	Clinical	3389 COVID-19, 1593 Non-COVID Img.	Separate DB	5-fold	NA	Supervised	Standard Preprocessing, VB-Net Toolkit for Segmentation, Lung Mask Generation	COVID-19 from Non-COVID-19	Lung Lesion-Oriented Method	3D ResNet34 (Classification), VB-Net (Segmentation)	Ensemble Learning	Grad-CAM	Acc=87.5,Sen=86.9, Spe=90.1,AUC=94.4, F1-Score=82.0
[102]	CT-Scan	Clinical	146 COVID-19, 149 Non-COVID Img.	135-20-140	Hold-out	NA	Supervised	Data Augmentation	COVID-19 from Non-COVID-19	Lung Region-Oriented Method	DenseNet (Classification)	Softmax	CAM	Acc=92,Sen=97,Spe=87, F1-Score=93
[103]	CT-Scan	Clinical	558 COVID-19 Patients	60%:20%:20%	5-fold	NA	Weakly-supervised learning	NA	COVID-19 from Other Pneumonia	NA	AD3D-MIL (Based on CNN)	NA	Proposed Loss Function	Dice=80.72,RVE=15.96
[104]	CT-Scan	Combination of Two Different DBs	1118 COVID-19, 96 Pneumonia, 107 Healthy Img.	70%:30%	Hold-out	NA	Supervised	Binary Mask, Lung Segmentation using Histogram Thresholding, Morphological Operation (Dilation, Hole Filling), and Removing All Small Connected Objects	COVID-19 from Other Pneumonia	Lung Region-Oriented Method	CNN	LSTM	NA	Acc=99.68
[105]	CT-Scan	Clinical	151 COVID-19, 498 Non-COVID Patients	490-82-77	Hold-out	NA	Supervised	Resizing, Padding, Data Augmentation	COVID-19 from Non-COVID-19	NA	CNN	Softmax	Visual Interpretation	AUC=70
[106]	CT-Scan	Combination of Two Different DBs	413 COVID-19, 439 Normal or Pneumonia Img.	50%:10%:40%	10-fold	ImageNet	Supervised	NA	COVID-19 from Non-COVID-19	NA	ResNet	Softmax	NA	Acc=93.01,Spe=94.77, Sen=91.45,Pre=95.18
[107]	CT-Scan	Clinical	73 COVID-19 Patients	NA	20-fold	NA	Supervised	Hyper-Parameter Tuning using MODE Algorithm	COVID-19 from Non-COVID-19	NA	CNN	NA	NA	Acc=92,F1-Score=90, Sen=90,Spe=90
[108]	CT-Scan	Clinical	98 COVID-19, 103 Non-COVID Patients	80%:10%:10%	Hold-out	NA	Supervised	Visual Inspection	COVID-19 from Non-COVID-19	NA	BigBiGAN	Linear	NA	AUC=97.2,Sen=92, Spe=91
[109]	CT-Scan	COVID-19 Set	470 COVID-19 Suspects	370-100	Hold-out	COPDGene	Supervised	Standardization, Re-scaling, Down Sampling, Zero padding	NA	Lung Region-Oriented Method	RTSU-Net (Based on RU-Net)	Sigmoid, Softmax	Upsampling	IOU=92.2,ASSD=86.6
[46]	CT-Scan	Clinical	79 COVID-19, 100 Common Pneumonia, 130 Patients without Pneumonia	378-50-130	5-fold	NA	Semi-supervised	Data Augmentation	NA	Lung Lesion-Oriented Method	AD3D-MIL (Based on CNN)	Bernouli Distributio n	CAM	Acc=97.9,AUC=99, F1-Score=97.9,Pre=97.9, Recall=97.9
[110]	CT-Scan	COVID-19 Clinical DB	150 COVID-19, 150 CAP, 150 NP Img.	80%:20%	5-fold	TCIA	Weakly-supervised	Data Augmentation, Fixed-Sized Sliding Window, Segmentation	COVID-19 from Other Pneumonia	Lung Region-Oriented Method	CNN (Classification), U-Net (Segmentation)	Softmax	Multi-Window Voting, Sequential Information Attention Module, CAM (Class Activation Maps), Categorical- Specific Joint Saliency	Acc=96.2,Pre=97.3, Sen=94.5,Spe=95.3, AUC=97
[47]	CT-Scan	COVID-SemiSeg	150 COVID-19, 150 CAP, 150 NP Img.	45-5-50	Hold-out	1600 CT images with pseudo labels	Semi-supervised	Pseudo Label Generation, Resizing	NA	Lung Lesion-Oriented Method	Semi-Supervised Inf-Net	Sigmoid	NA	Dice=73.9,Sen=72.5, Spe=96,MAE=6.4
[45]	CT-Scan	Clinical	1315 COVID-19, 3342 Non-COVID	3997- 60 - 600	5-fold	NA	Weakly-	Lobe Segmentation, Cropping,	COVID-19 from	Lung Region-	3D-ResNets	Softmax	Heatmap Visualization	Acc=93.3,Sen=87.6,

			Img.				supervised	Resizing, Data Augmentation	Other Pneumonia	Oriented Method	(Classification), 3d-U-Net (Segmentation)			Spe=95.5
[52]	CT-Scan	Clinical	296 COVID-19, 1735 CAP, 1325 Non-Pneumonia Img.	Separate DB	NA	NA	Supervised	Lung Segmentation using U-net	COVID-19 from Other Pneumonia	Lung Region-Oriented Method	COVNet (Classification, Based on ResNet), U-Net (Segmentation)	Softmax	Grad-CAM	AUC=96,Sen=90, Spe=96
[111]	CT-Scan	Clinical	1266 COVID-19, 4106 Lung Cancer Patients	Separate DB	NA	Clinical	Supervised	Lung Segmentation, 3-Dimensional Bounding Box, Non-Lung Area Suppression Operation	COVID-19 from Other Pneumonia	Lung Region-Oriented Method	DenseNet (Segmentation), COVID-19Net (Classification)	Sigmoid	Combining Feature Vectors, Multivariate Cox Proportional Hazard Model, Visualizations	Acc=81.24,AUC=0.90, Sen=78.93,Spe=89.93, F1-Score=86.92
[20]	CT-Scan	Clinical	521 COVID-19, 665 Non-COVID Patients	70%:20%:10%	Hold-out	ImageNet	Supervised	Lung Segmentation using Thresholding and The Manual Active Contour Segmentation Method, Padding, Resizing, Lung windowing, Normalization, Standardization	COVID-19 from Non-COVID-19	Lung Region-Oriented Method	EfficientNet B4	Sigmoid	Generating Heat Map	Acc=96,Sen=95, Spec=96
[112]	CT-Scan	Combination of Two Different DBs	1272 COVID-19,1230 Non-COVID Img.	70%:30%	5-fold and 10-fold	NA	Semi-supervised	Normalization, Standardization.	COVID-19 from Non-COVID-19	Lung Region-Oriented Method	PQIS-Net (Segmentation)	Majority Voting	Patch-Based Classification on Segmented Lung CT Images	Acc=93.1,Pre=89, Recall=83.5,F1-Score=82.6,AUC=98.2
[113]	CT-Scan	Combination of Different DBs	1194 COVID-19, 1357 Non-COVID Pneumonia, 1442 Nonpneumonia Img.	80%:20%	Hold-out	ImageNet	Supervised	Converting to One-channel Grayscale PNG Images, Rescaling, Normalizing, Data Augmentation	COVID-19 from Other Pneumonia	NA	ResNet-50	Softmax	Grad-CAM	Acc=99.87,Spec=100, Sen=99.58
[48]	CT-Scan	Clinical DB, SPIE-AAPM-NCI	111 COVID-19, 115 CAP, 109 Normal Patients	300-15-20	Hold-out	NA	Supervised	Generating Pseudo-Infection Anomalies using Perlin Noise, Resampling, Resizing, Normalization	COVID-19 from Other Pneumonia	Lung Lesion-Oriented Method	BCDU-Net (Segmentation), CNN (Classification)	NA	NA	Acc=86.66,Spec=100, Sen=90.91
[114]	CT-Scan	Clinical	255 COVID-19, 420 Typical Viral Pneumonia Img.	Separate DB	Hold-out	ImageNet	Supervised	Converting to Grayscale, Grayscale Binarization, Background Area Filling, Reverse Color, Cropping To Obtain ROI Images	COVID-19 from Non-COVID-19	NA	M-inception (Based on GoogleNet Inception-V3)	Softmax	NA	Acc=79.3,Spec=83, Sen=67,AUC=81,F1-Score = 63
[115]	CT-Scan	Clinical	51 COVID-19 Patients, 55 Patients with Other Diseases	Separate DB	Hold-out	ImageNet	Supervised	NA	NA	Lung Lesion-Oriented Method	UNet++ (Based on ResNet-50)	NA	NA	Acc=96,Spec=94, Sen=98,PPV=94.23, NPV=97.92
[116]	CT-Scan	Clinical	777 COVID-19, 505 Bacteria Pneumonia, 708 Normal Img.	60%:10%:30%	Hold-out	ImageNet	Supervised	Lung Detection, Filling the Blank Area of Image with Its Rotational Lung Areas	COVID-19 from Other Pneumonia	NA	DRENet (Based on ResNet-50 and FPN)	NA	Grad-CAM	Pre=93,Recall=93, Acc=93,Spec=93, F1-Score=93
[117]	CT-Scan	Mosmed Dataset	1100 COVID-19, 1980 Normal Img.	1980-1100	NA	ImageNet	Supervised	Resizing, Random Crops	COVID-19 from Non-COVID-19	NA	ResNet-50	Majority Voting	NA	Acc=96,AUC=90, Sen=100,Spec=96
[118]	CT-Scan	COVID-CTx	324 COVID-19, 504 Normal Img.	60%:20%:20%	3-fold	NA	Supervised	Resizing, Lung Segmentation, K-means Clustering, Contrast Enhancement, Morphological Closing, Hole Filling, Data Augmentation	COVID-19 from Non-COVID-19	Lung Region-Oriented Method	AM-SdenseNet (classification), U-Net (Segmentation)	Sigmoid	NA	Acc=99.18,Pre=99.32, Recall=98.97,F1-score=91.14
[119]	CT-Scan	Combination of Two Different DBs	1601 COVID-19, 1626 Non-COVID Img.	80%:20%	Hold-out	NA	Supervised	NA	COVID-19 from Non-COVID-19	NA	EfficientNet and Convolutinal Block Attention Module (CBAM)	SVM	NA	Acc=98, Pre=98,Sen=98, F1-score=98
[120]	CT-Scan	Combination of Two Different DBs	259 COVID-19, 171 Non-COVID-19 Patients	NA	10-fold	DeepLesi LIDC-IDRI	Supervised	Image Resize, Image Augmentation (Resizing, Random Flipping, Random Cropping, Color Distortions)	COVID-19 from Non-COVID-19	NA	Prototypical Network	Relu	NA	Acc=88.5,Pre=89.9, Recall=88.6,AUC=94.5
[121]	CT-Scan, X-ray	Combination of Two Different DBs	3065 COVID-19, 3065 Non-COVID Img.	70%:30%	NA	NA	Supervised	Data Augmentation	COVID-19 from Non-COVID-19	NA	ConvLSTM	NA	NA	Acc=98.45,F1-score=98.07,Mcc=96.81
[51]	CT-Scan, X-ray	Combination of Two Different DBs	2780 Bacterial Pneumonia, 1493 Viral Pneumonia, 231 COVID-19, 1583 Normal Img.	80%:20%	NA	ImageNet	Supervised	Intensity Normalization, CLAHE Method, DA, Resizing	COVID-19 from Other Pneumonia	Lung Region-Oriented Method	U-Net (Segmentation), Inception ResNetV2 (Classification)	MLP	NA	Acc=92.18,Sen=92.11, Spec=96.06,Pre=92.38, F1-Score=92.07

The work carried out by Shazia et al. [16] states that applying deep learning techniques to radiological images for novel coronavirus identification has the potential to reduce the workload of medical practitioners and increase the accuracy and efficiency of COVID-19 diagnosis. In what follows, we discuss the reviewed articles on developing DL models for the early diagnosis of COVID-19 using medical images, and attempt to answer these research questions: What are the most commonly used DL techniques for COVID-19 detection using medical images? What challenges may we face during the deep neural network training process on chest images, and how can we cope with them? What are the advantages and disadvantages of each imaging modality in classification and segmentation tasks?

5.1. Deep neural networks for COVID-19 diagnosis

A revolution in image processing and machine vision has taken place with the advent of deep learning techniques [122]. Deep neural networks have been used in the domain of image processing to solve difficult problems including image classification, detection, and segmentation [123]. These networks eliminate the need for manual feature extraction. They have introduced the concept of end-to-end learning by receiving annotated images as input and discovering the underlying patterns in each image class automatically [124]. A convolutional neural network can have hundreds of layers where each layer learns to detect different image features. DNNs have also achieved great success in analyzing medical images by providing high accuracy, stability, scalability, and efficiency [125]. They can provide Health professionals with more details about the internal organs and patient's tissues, and help physicians diagnose many types of disease, such as pneumonia, brain injuries, cancer, internal bleeding, and pneumonia, brain injuries, cancer, internal bleeding, etc [126]. Not only in medical image analysis for the diagnosis of such diseases but also during the recent COVID-19 pandemic, deep learning has proved its success [25]. Gaur et al. [127] give evidence on the successful application of deep learning techniques for COVID-19 infection detection. Their work confirms that deep machine vision models can be implemented in the healthcare sector to screen and detect COVID-19 from chest X-rays. Sethi et al. [128] also utilize different deep CNN architectures to provide doctors with diagnosis recommendations for COVID-19. They show that CNN-based architectures have the potential to diagnose COVID-19 disease using chest X-ray Images.

A variety of deep neural networks developed for COVID-19 diagnosis purposes is shown in Figure 11. This figure also shows which classifiers and how many times have been used in each DNN. Due to using different datasets with different sizes and properties, a direct comparison between deep networks

considering performance metrics is not possible. However, based on our review, Res-Net and VGG are the most common networks used in classification tasks, and for segmentation tasks, various versions of U-Net deep neural networks have been utilized.

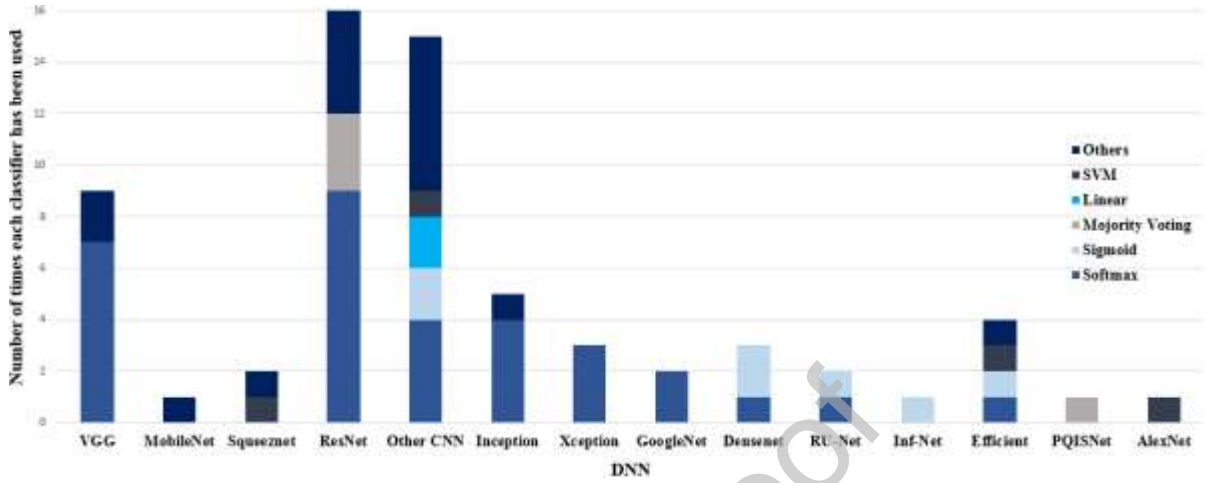

Fig. 11. Number of times that each pair of DNNs and classifiers has been used in reviewed papers for COVID-19 diagnosis.

Different experimental studies have proved good results of the state-of-the-art deep architectures VGG and ResNet for challenging recognition and localization problems such as image segmentation [129]. The main advantage of VGG architecture is its good generalization ability in new datasets [130]. In the 2014-ILSVRC competition, VGG became famous, despite being in 2nd place, due to its simplicity, homogenous topology, and increased depth [129]. On the other hand, ResNet can prevent the degradation problem of deep CNNs. This problem occurs when the accuracy gets saturated and quickly degrades with network depth increasing [131]. ResNet has shortcut connections that skip one or more layers and facilitate deep network training without adding extra parameters or computational complexity. ResNet also lets feature maps from the initial layers that usually include fine details easily propagate to the deeper layers [132].

It is clear also from Figure 11 that the majority of works have utilized the Softmax classifier in their models. As mentioned before, this classifier represents a probability distribution over class labels, and its output can be directly displayed. Besides, since output values are between 0 and 1, they can be directly fed into any other model without the need for normalization.

It is worth mentioning that using different pre-processing approaches, diverse classifiers, applying the transfer learning method, and other techniques employed for compensating for data shortage could directly affect the results of DNNs. A sufficient number of clinically annotated data is critical for the training step. However, there are very few clinical datasets on COVID-19 which are publicly available

and these datasets contain a limited number of COVID-19 cases. Several reviewed studies [20,23,81–87,105,39,47,53,76–80] have applied transfer learning and image preprocessing techniques such as image augmentation or used a combination of different datasets to overcome the COVID-19 data leakage and data imbalance problems and enhance their performance. However, these approaches may lead to high variance estimation of deep learning models' performance during the test phase [133]. Since many of the COVID-19 prediction models are poorly reported, and at high risk of bias and model overfitting [134], more investigation will be needed to ensure the performance of these models in clinical use.

5.2. Classification and segmentation techniques for COVID-19 diagnosis

Figure 12 shows the total number of studies conducted in the field of segmentation and/or classification for diagnosing COVID-19 patients. Based on the results of this figure, most studies have only focused on the classification task. As mentioned before, we categorized COVID-19 classification approaches into two main classes named COVID-19 from Non-COVID, and COVID-19 from Other Pneumonia, which respectively refer to two-class and multi-class classifications. Although the differentiation of COVID-19 from other types of pneumonia is sometimes challenging, an equal number of studies have modeled the COVID-19 diagnosis problem as a two-class and multi-class classification task. Some researchers have also taken advantage of both classification and segmentation techniques to improve model accuracy. These models first extract the ROI (Region of Interest) of the image in the pre-processing phase and then search within the ROI region instead of the whole region. However, most classification works have preferred to process the whole of the image rather than the ROI region. The main reason is that annotating COVID-19 medical images for a segmentation task is difficult and time-consuming for clinicians.

5.3. Imaging modalities for COVID-19 diagnosis

The most common imaging modalities for COVID-19 infection identification are CT scan, Lung Ultrasound (LUS), and Chest X-ray radiography. The chest X-ray is low cost, easy to perform, and has low radiation. It also is fast and immediately available for radiologist analysis; the last feature has made it one of the first imaging modalities during the COVID-19 pandemic [135]. Nevertheless, it has limited sensitivity in detecting lung lesions in the early stages of infections [136]. While the Chest CT, being a rapid imaging procedure, may be more sensitive and accurate for the early diagnosis of COVID-19, it

exposes patients to more radiation than typical X-rays. Moreover, it is time-consuming for radiologists to diagnose COVID-19 from CT-scan images (about 21.5 minutes for experienced ones). After each patient, CT scanners will need to be sanitized which is a time-consuming, tedious, and expensive process [137,138].

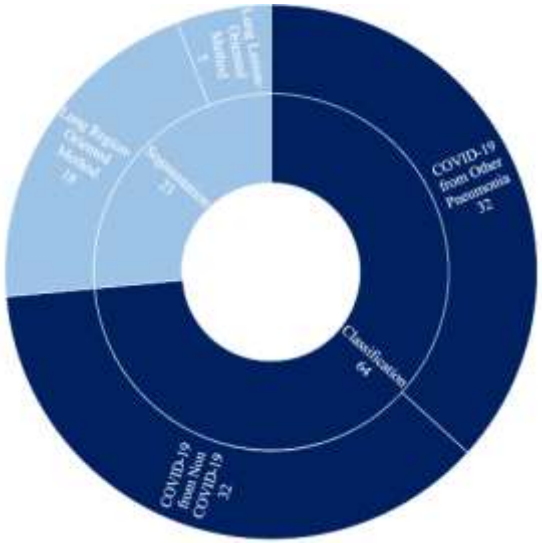

Fig. 12. Total number of research works conducted in COVID-19 classification and segmentation, and number of studies done in each sub-class.

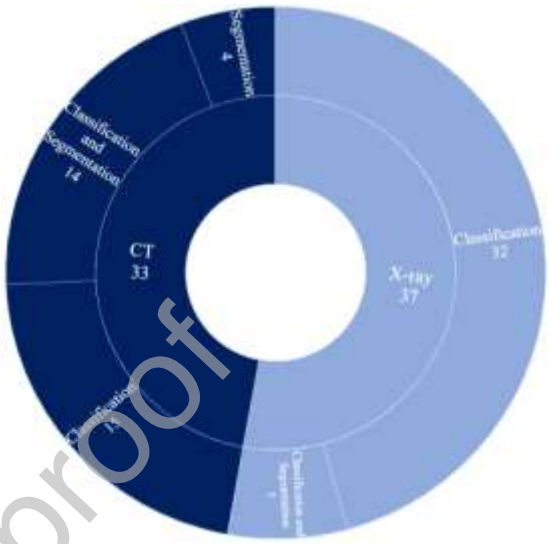

Fig. 13. Total number of studies conducted on each modality, and number of classification and segmentation works done for each modality.

Compared to the other two modalities, chest ultrasound is low-cost and radiation-free. It can accurately detect the location of objects in real-time and be applied to different lung diseases [139]. Ultrasound has a low false-negative rate in COVID-19 diagnosis [140]. All COVID-19 abnormalities which are visible in CT scan images are also presented on ultrasound images just as clearly [141]. Its accuracy in identifying lung pathologies is better than Chest X-ray, it also is portable, safe, non-invasive, repeatable, and easy to use [136]. However, it shows low sensitivity in comparison to chest X-rays, and it cannot detect deep and intrapulmonary lesions [142].

In the absence of a CT scan, a chest MRI could be recommended for suspected or confirmed COVID-19 patients. Although MRI has low anatomic resolution and is in danger of inevitable artifacts because of breathing motion, its ability to visualize variations in lung structure is constantly evolving [143].

Some other imaging techniques have also been utilized for the COVID-19 diagnosis such as Hyperspectral Imaging (HSI), Scanning Electron Microscopy (SEM), and Positron Emission Tomography (PET). HSI is a medical imaging technique that offers noninvasive disease diagnosis. HSI, also known as Imaging Spectroscopy, can capture spectral information for multiple wavelengths at

each image pixel [144]. The maximum contrast in hyperspectral imaging is related to the maximum particle concentration [145]. The main disadvantages of hyperspectral imaging are its cost and complexity. To analyze hyperspectral data, fast computers, sensitive detectors, and large data storage capacities are required.

SEM is a powerful tool for infectious disease diagnosis and scans the sample surface morphology by bright focused electron beam emission [146]. It can produce high-resolution and high-quality images that reveal complex and delicate structures. However, it has several cons. In this technique, samples must always be in a vacuum, so this technique cannot be used for live specimens. Electron microscopes are large and need plenty of space in a laboratory. They also are high-sensitive and could be affected by magnetic fields and vibrations of other lab equipment. Artifacts may be present in SEM images and need to be avoided [147].

PET is a type of nuclear medicine imaging. It applies a small amount of radioactive material to visualize and measure variations in metabolic processes. This non-invasive approach can display very early changes in the cells. Despite the advantages of the PET approach, it is not a routine examination for COVID-19 diagnosis because of its low global accessibility, high inspection cost, complex scanning procedures, and concurrent risks of virus spreading.

Considering the importance and the role of CT and X-ray chest images in diagnosing COVID-19 patients, our review has investigated machine vision-based techniques developed in the literature for the early diagnostics of COVID-19 and other types of pneumonia using these imaging modalities. Figure 13 illustrates the total number of research works reviewed for each one. It also shows the number of classification and segmentation tasks conducted for each modality. As one can see, most researchers have selected to work on the X-ray modality. Also, the combination of CT-Scan and segmentation in the diagnosis of COVID-19 patients is more common than X-ray and segmentation. The reason is that CT-Scan produces a 3D view of the chest region and allows for a more detailed view compared to X-ray. Most X-ray modality-based studies have focused on classification for COVID-19 diagnosis, which is a less challenging task.

6. Challenges

Deep learning approaches require a large amount of data to build a robust predictive model. However, COVID-19 is a new infectious disease, and the lack of large-scale labeled data is the main challenge in this area. It might lead to overfitting and reduce the accuracy of DL-based models. To

overcome this challenge, a majority of works [23,39,53,76–87] have combined several public datasets to compensate for the scarcity of well-annotated datasets of appropriate size. However, duplication of images across these datasets is a potential risk during data combination tasks.

Transfer learning is another technique to cope with overfitting and data shortage problems. It is more likely to have a more accurate model by fine-tuning the pre-trained model than training the model from scratch on a small dataset [79,80,148]. Some studies [20,47,49,51,82,115] have used transfer learning to effectively train models on relatively small labeled datasets in COVID-19 segmentation tasks. However, they have mostly applied deep neural networks pre-trained on the ImageNet dataset which includes images that are entirely different from chest images. A small number of segmentation tasks have also used chest images with pseudo labels for the pre-training stage [47]. Preparing noisy labels for the segmentation task is much easier than obtaining clean annotations at the pixel level. Consequently, some research works have attempted to develop a framework to learn from noisy label images [46].

Class imbalance is another main issue in COVID-19 diagnosis since the number of data related to COVID-19 is much less than other pneumonia diseases. Several works [23,39,69,71,72,102,105] applied data augmentation methods to compensate for the small COVID-19 datasets and avoid unbalancing data problems. Also, some researchers [23,77,81,87] used the Generative Adversarial Network (GAN) framework in the pre-processing phase to generate synthetic images to deal with this problem.

Most of the COVID-19 images compress into Non-DICOM formats leading to quality loss. Since the quality of public health information is essential for health monitoring, the lack of image quality remains a challenge in the COVID-19 diagnosis problem. The work carried out by Harmon et al. [99] has reconstructed CT images by super-resolution technique to achieve better accuracy. This technique improves the accuracy of algorithms by making enhanced images with higher contrast.

Generally, lung segmentation can improve the accuracy of a classification task and reduce misdiagnosis [149]. As mentioned before, we grouped the COVID-19 segmentation approaches into two main categories, named the lung-region-oriented methods and the lung-lesion-oriented methods. Lesion detection is a challenging task in the medical imaging area as the lesion size is small in comparison to the whole lung size. In addition, the shape of lesions and their texture and location are very diverse. Most works [110,150–152] applied U-Net architecture or Attention-based U-Net to

segment lesions and lung regions in COVID-19 automatic detection tasks. Another challenging task is to discriminate COVID-19 from other types of viral pneumonia since COVID-19 is similarly caused by an infective agent. Several DL-based models have been developed in the literature to distinguish between them [53,70].

7. Recommendations

The awareness and knowledge of the different clinical features of COVID-19 are essential in the early diagnosis and management of the recent pandemic. Some studies were conducted to compare the clinical presentations of COVID-19 patients versus patients infected with other types of pneumonia [153–157]. Researchers found that considering a combination of information such as background and clinical findings of patients, the duration of the symptoms, ancillary imaging findings, and follow-up CT-Scan imaging when needed would be helpful in the differential diagnosis [154]. Based on this, we strongly recommend developing DL-based models that utilize clinical text data, as well as CT and X-ray images to provide a more accurate diagnosis of COVID-19. While many DL-based techniques have been proposed in the literature for detecting COVID-19 patients based on X-ray images, CT-scan images, or both, less work is being done on diagnosis and prediction using clinical text data. Moreover, to the best of our knowledge, there is no research work in the literature focusing on COVID-19 diagnosis based on both medical images and textual data.

As we mentioned before, dealing with small-size datasets is the main challenge in the COVID-19 diagnosis area which can lead to overfitting and reduce the model generalization performance. Researchers may address this problem through various model enhancement and data generation techniques. Since more complex models with more hyper-parameters are more overfitting-prone than shallower ones, the adaptation of model complexity to the complexity of data can help researchers overcome the issue of overfitting [158]. Another effective way to have more accurate predictions is combining the results of multiple models, which is called ensemble learning [159]. This approach involves several individual models combined in some way such as weighted averaging, and voting. The ensemble model obtains better generalization performance compared to any of the individual models.

Data imbalance is another main issue in diagnosing COVID-19 patients which can undermine model predictability. The oversampling methods can alleviate both data scarcity and data imbalance problems [160]. One approach to oversampling is generating synthetic samples using augmentation techniques such as GAN.

8. Conclusion

COVID-19 has spread dramatically in a short time around the world. The SARS-CoV-2 infection causes symptoms from weak to severe in different people, and to date, more than 6.5 million deaths have been reported to WHO (https://covid19.who.int). Early diagnosis of COVID-19 can help to prevent the spread of this pneumonia, and save many lives. Although the standard test for COVID-19 diagnosis is RT-PCR, this test is time-consuming, and it is possible to show false-negative results [161]. Therefore, many researchers applied deep learning models to detect COVID-19 in the early stage using X-ray and CT images. Chest imaging has a useful role in the detection and management of COVID-19, even in the early stage of the disease. It helps in suspected patients' identification, Breaking the disease transmission chain, and preventing the further spread of infection [115]. Deep learning approaches can extract rich features from chest images. They are capable of interpreting medical images and distinguishing different types of pneumonia. Physicians can predict COVID-19, estimate its severity, and extract and interpret the infected region by the data extracted from these networks [67].

During the course of this study, we have undertaken a comprehensive review of some 60 papers that have appeared in the literature on the subject of deep learning-based COVID-19 segmentation and classification using X-ray and CT images. We reported the informative details of each model proposed in the reviewed papers. We also listed the public datasets for diagnosing COVID-19 patients and provided several charts summarizing various techniques used in the different phases of developing a DL-based diagnostic model for COVID-19.

Finally, we discussed the challenges in the research on COVID-19 diagnosis based on medical imaging. We found that the reviewed models are at high risk of bias especially because of the overfitting problem, and their generalization performance is therefore unreliable. Consequently, none of these models are recommended for clinical use. Since the scarcity of large-scale public annotated datasets is one of the main challenges leading to overfitting, the compilation, curating, and sharing of well-annotated datasets is urgently needed in order to develop and validate more accurate models for diagnosing COVID-19.

Competing interests: None declared

Funding: None

Ethical approval: Not required

References

[1] Mei X, Lee H-C, Diao K, Huang M, Lin B, Liu C, et al. Artificial intelligence–enabled rapid diagnosis of patients with COVID-19. Nat Med 2020;26:1224–8. https://doi.org/10.1038/s41591-020-0931-3.

[2] Ye Z, Zhang Y, Wang Y, Huang Z, Song B. Chest CT manifestations of new coronavirus disease 2019 (COVID-19): a pictorial review. Eur Radiol 2020;30:4381–9. https://doi.org/10.1007/s00330-020-06801-0.

[3] Rodriguez-Morales AJ, Cardona-Ospina JA, Gutiérrez-Ocampo E, Villamizar-Peña R, Holguin-Rivera Y, Escalera-Antezana JP, et al. Clinical, laboratory and imaging features of COVID-19: A systematic review and meta-analysis. Travel Med Infect Dis 2020;34:101623. https://doi.org/10.1016/j.tmaid.2020.101623.

[4] Bai HX, Hsieh B, Xiong Z, Halsey K, Choi JW, Tran TML, et al. Performance of Radiologists in Differentiating COVID-19 from Non-COVID-19 Viral Pneumonia at Chest CT. Radiology 2020;296:E46–54. https://doi.org/10.1148/radiol.2020200823.

[5] Luz E, Silva P, Silva R, Silva L, Guimarães J, Miozzo G, et al. Towards an effective and efficient deep learning model for COVID-19 patterns detection in X-ray images. Res Biomed Eng 2021. https://doi.org/10.1007/s42600-021-00151-6.

[6] Haque KF, Abdelgawad A. A Deep Learning Approach to Detect COVID-19 Patients from Chest X-ray Images. AI 2020;1:418–35. https://doi.org/10.3390/ai1030027.

[7] Alom MZ, Taha TM, Yakopcic C, Westberg S, Sidike P, Nasrin MS, et al. A State-of-the-Art Survey on Deep Learning Theory and Architectures. Electronics 2019;8. https://doi.org/10.3390/electronics8030292.

[8] Kaur M, Kumar V, Yadav V, Singh D, Kumar N, Das NN. Metaheuristic-based Deep COVID-19 Screening Model from Chest X-ray Images. J Healthc Eng 2021;2021:8829829. https://doi.org/10.1155/2021/8829829.

[9] Iandola FN, Han S, Moskewicz MW, Ashraf K, Dally WJ, Keutzer K. SqueezeNet: AlexNet-level accuracy with 50x fewer parameters and < 0.5 MB model size. ArXiv Prepr ArXiv160207360 2016.

[10] Deng J, Dong W, Socher R, Li L-J, Li K, Fei-Fei L. Imagenet: A large-scale hierarchical image database. 2009 IEEE Conf. Comput. Vis. pattern Recognit., Ieee; 2009, p. 248–55.

[11] Alom MZ, Taha TM, Yakopcic C, Westberg S, Sidike P, Nasrin MS, et al. A State-of-the-Art Survey on Deep Learning Theory and Architectures. Electronics 2019;8. https://doi.org/10.3390/electronics8030292.

[12] Zabbah I, Layeghi K, Ebrahimpour R. Improving the Diagnosis of COVID-19 by using a combination of Deep Learning Models. J Electr Comput Eng Innov 2022;10:411–24. https://doi.org/10.22061/jecei.2022.8200.491.

[13] Yang D, Martinez C, Visuña L, Khandhar H, Bhatt C, Carretero J. Detection and analysis of COVID-19 in medical images using deep learning techniques. Sci Rep 2021;11:19638. https://doi.org/10.1038/s41598-021-99015-3.

[14] Sinha D, El-Sharkawy M. Thin MobileNet: An Enhanced MobileNet Architecture. 2019 IEEE 10th Annu. Ubiquitous Comput. Electron. Mob. Commun. Conf., 2019, p. 280–5. https://doi.org/10.1109/UEMCON47517.2019.8993089.

[15] Alzubaidi L, Zhang J, Humaidi AJ, Al-Dujaili A, Duan Y, Al-Shamma O, et al. Review of deep learning: concepts, CNN architectures, challenges, applications, future directions. J Big Data 2021;8:53. https://doi.org/10.1186/s40537-021-00444-8.

[16] Shazia A, Xuan TZ, Chuah JH, Usman J, Qian P, Lai KW. A comparative study of multiple neural network for detection of COVID-19 on chest X-ray. EURASIP J Adv Signal Process 2021;2021:50. https://doi.org/10.1186/s13634-021-00755-1.

[17] Alzubaidi L, Zhang J, Humaidi AJ, Al-Dujaili A, Duan Y, Al-Shamma O, et al. Review of deep learning: concepts, CNN architectures, challenges, applications, future directions. J Big Data 2021;8:53. https://doi.org/10.1186/s40537-021-00444-8.

[18] Karim M, Döhmen T, Rebholz-Schuhmann D, Decker S, Cochez M, Beyan O. DeepCOVIDExplainer: Explainable COVID-19 diagnosis based on chest X-ray images. ArXiv Prepr ArXiv200404582 2020.

[19] Pachade S, Porwal P, Kokare M, Giancardo L, Mériaudeau F. NENet: Nested EfficientNet and adversarial learning for joint optic disc and cup segmentation. Med Image Anal 2021;74:102253. https://doi.org/10.1016/j.media.2021.102253.

[20] Bai HX, Wang R, Xiong Z, Hsieh B, Chang K, Halsey K, et al. Artificial Intelligence

Augmentation of Radiologist Performance in Distinguishing COVID-19 from Pneumonia of Other Origin at Chest CT. Radiology 2020;296:E156–65. https://doi.org/10.1148/radiol.2020201491.
[21] Siddique N, Paheding S, Elkin CP, Devabhaktuni V. U-Net and Its Variants for Medical Image Segmentation: A Review of Theory and Applications. IEEE Access 2021;9:82031–57. https://doi.org/10.1109/ACCESS.2021.3086020.
[22] Ahmed I, Chehri A, Jeon G. A Sustainable Deep Learning-Based Framework for Automated Segmentation of COVID-19 Infected Regions: Using U-Net with an Attention Mechanism and Boundary Loss Function. Electronics 2022;11. https://doi.org/10.3390/electronics11152296.
[23] Waheed A, Goyal M, Gupta D, Khanna A, Al-Turjman F, Pinheiro PR. CovidGAN: Data Augmentation Using Auxiliary Classifier GAN for Improved COVID-19 Detection. IEEE Access 2020;8:91916–23. https://doi.org/10.1109/ACCESS.2020.2994762.
[24] Roy S, Menapace W, Oei S, Luijten B, Fini E, Saltori C, et al. Deep Learning for Classification and Localization of COVID-19 Markers in Point-of-Care Lung Ultrasound. IEEE Trans Med Imaging 2020;39:2676–87. https://doi.org/10.1109/TMI.2020.2994459.
[25] Lu W, Zhang S, Chen B, Chen J, Xian J, Lin Y, et al. A Clinical Study of Noninvasive Assessment of Lung Lesions in Patients with Coronavirus Disease-19 (COVID-19) by Bedside Ultrasound TT - Nicht-invasive Beurteilung von pulmonalen Läsionen bei Patienten mit Coronavirus-Erkrankung (COVID-19) durch Ultrasch. Ultraschall Med 2020;41:300–7.
[26] Huang Y, Wang S, Liu Y, Zhang Y, Zheng C, Zheng Y, et al. A preliminary study on the ultrasonic manifestations of peripulmonary lesions of non-critical novel coronavirus pneumonia (COVID-19) 2020. https://doi.org/10.21203/rs.2.24369/v1.
[27] Sofia S, Boccatonda A, Montanari M, Spampinato M, D'ardes D, Cocco G, et al. Thoracic ultrasound and SARS-COVID-19: a pictorial essay. J Ultrasound 2020;23:217–21. https://doi.org/10.1007/s40477-020-00458-7.
[28] Zu ZY, Jiang M Di, Xu PP, Chen W, Ni QQ, Lu GM, et al. Coronavirus Disease 2019 (COVID-19): A Perspective from China. Radiology 2020;296:E15–25. https://doi.org/10.1148/radiol.2020200490.
[29] Punn NS, Agarwal S. Automated diagnosis of COVID-19 with limited posteroanterior chest X-ray images using fine-tuned deep neural networks. Appl Intell 2020. https://doi.org/10.1007/s10489-020-01900-3.
[30] Srivastava N, Hinton G, Krizhevsky A, Sutskever I, Salakhutdinov R. Dropout: A Simple Way to Prevent Neural Networks from Overfitting. J Mach Learn Res 2014;15:1929–1958.
[31] Hawkins DM. The Problem of Overfitting. J Chem Inf Comput Sci 2004;44:1–12. https://doi.org/10.1021/ci0342472.
[32] Ng AY. Preventing "Overfitting" of Cross-Validation Data. Proc. Fourteenth Int. Conf. Mach. Learn., San Francisco, CA, USA: Morgan Kaufmann Publishers Inc.; 1997, p. 245–253.
[33] Bengio Y, Grandvalet Y. No Unbiased Estimator of the Variance of K-Fold Cross-Validation. J Mach Learn Res 2004;5:1089–1105.
[34] Yadav S, Shukla S. Analysis of k-Fold Cross-Validation over Hold-Out Validation on Colossal Datasets for Quality Classification. 2016 IEEE 6th Int. Conf. Adv. Comput., 2016, p. 78–83. https://doi.org/10.1109/IACC.2016.25.
[35] Kohavi R. A study of cross-validation and bootstrap for accuracy estimation and model selection. Ijcai, vol. 14, 1995, p. 1137–45.
[36] Bryll R, Gutierrez-Osuna R, Quek F. Attribute bagging: improving accuracy of classifier ensembles by using random feature subsets. Pattern Recognit 2003;36:1291–302. https://doi.org/https://doi.org/10.1016/S0031-3203(02)00121-8.
[37] Pan SJ, Yang Q. A Survey on Transfer Learning. IEEE Trans Knowl Data Eng 2010;22:1345–59. https://doi.org/10.1109/TKDE.2009.191.
[38] Torrey LA, Shavlik J. Chapter 11 Transfer Learning, 2009.
[39] Brunese L, Mercaldo F, Reginelli A, Santone A. Explainable Deep Learning for Pulmonary Disease and Coronavirus COVID-19 Detection from X-rays. Comput Methods Programs Biomed 2020;196:105608. https://doi.org/https://doi.org/10.1016/j.cmpb.2020.105608.
[40] Khalid PM, Amin BS. SARS n-CoV2-19 detection from chest X-ray images using deep neural networks. Int J Pervasive Comput Commun 2020;16:419–27. https://doi.org/10.1108/IJPCC-06-2020-0060.
[41] Cunningham P, Cord M, Delany SJ. Supervised Learning BT - Machine Learning Techniques for Multimedia: Case Studies on Organization and Retrieval. In: Cord M, Cunningham P, editors., Berlin, Heidelberg: Springer Berlin Heidelberg; 2008, p. 21–49. https://doi.org/10.1007/978-3-540-75171-7_2.
[42] Ghahramani Z. Unsupervised Learning BT - Advanced Lectures on Machine Learning: ML

Summer Schools 2003, Canberra, Australia, February 2 - 14, 2003, Tübingen, Germany, August 4 - 16, 2003, Revised Lectures. In: Bousquet O, von Luxburg U, Rätsch G, editors., Berlin, Heidelberg: Springer Berlin Heidelberg; 2004, p. 72–112. https://doi.org/10.1007/978-3-540-28650-9_5.

[43] Zhou Z-H. A brief introduction to weakly supervised learning. Natl Sci Rev 2018;5:44–53. https://doi.org/10.1093/nsr/nwx106.

[44] Zhai X, Oliver A, Kolesnikov A, Beyer L. S4L: Self-Supervised Semi-Supervised Learning. Proc. IEEE/CVF Int. Conf. Comput. Vis., vol. abs/1905.0, 2019, p. 1476–85.

[45] Wang J, Bao Y, Wen Y, Lu H, Luo H, Xiang Y, et al. Prior-Attention Residual Learning for More Discriminative COVID-19 Screening in CT Images. IEEE Trans Med Imaging 2020;39:2572–83. https://doi.org/10.1109/TMI.2020.2994908.

[46] Wang G, Liu X, Li C, Xu Z, Ruan J, Zhu H, et al. A Noise-Robust Framework for Automatic Segmentation of COVID-19 Pneumonia Lesions From CT Images. IEEE Trans Med Imaging 2020;39:2653–63. https://doi.org/10.1109/TMI.2020.3000314.

[47] Fan D-P, Zhou T, Ji G-P, Zhou Y, Chen G, Fu H, et al. Inf-Net: Automatic COVID-19 Lung Infection Segmentation From CT Images. IEEE Trans Med Imaging 2020;39:2626–37. https://doi.org/10.1109/TMI.2020.2996645.

[48] Javaheri T, Homayounfar M, Amoozgar Z, Reiazi R, Homayounieh F, Abbas E, et al. CovidCTNet: an open-source deep learning approach to diagnose COVID-19 using small cohort of CT images. Npj Digit Med 2021;4:29. https://doi.org/10.1038/s41746-021-00399-3.

[49] Rajaraman S, Siegelman J, Alderson PO, Folio LS, Folio LR, Antani SK. Iteratively Pruned Deep Learning Ensembles for COVID-19 Detection in Chest X-rays. IEEE Access 2020;8:115041–50. https://doi.org/10.1109/ACCESS.2020.3003810.

[50] Duran-Lopez L, Dominguez-Morales JP, Corral-Jaime J, Vicente-Diaz S, Linares-Barranco A. COVID-XNet: A Custom Deep Learning System to Diagnose and Locate COVID-19 in Chest X-ray Images. Appl Sci 2020;10:5683. https://doi.org/https://doi.org/10.3390/app10165683.

[51] El Asnaoui K, Chawki Y. Using X-ray images and deep learning for automated detection of coronavirus disease. J Biomol Struct Dyn 2020:1–12. https://doi.org/10.1080/07391102.2020.1767212.

[52] Li L, Qin L, Xu Z, Yin Y, Wang X, Kong B, et al. Using Artificial Intelligence to Detect COVID-19 and Community-acquired Pneumonia Based on Pulmonary CT: Evaluation of the Diagnostic Accuracy. Radiology 2020;296:E65–71. https://doi.org/10.1148/radiol.2020200905.

[53] Mahmud T, Rahman MA, Fattah SA. CovXNet: A multi-dilation convolutional neural network for automatic COVID-19 and other pneumonia detection from chest X-ray images with transferable multi-receptive feature optimization. Comput Biol Med 2020;122:103869. https://doi.org/https://doi.org/10.1016/j.compbiomed.2020.103869.

[54] Nwankpa C, Ijomah W, Gachagan A, Marshall S. Activation Functions: Comparison of trends in Practice and Research for Deep Learning 2018.

[55] Noble WS. What is a support vector machine? Nat Biotechnol 2006;24:1565—1567. https://doi.org/10.1038/nbt1206-1565.

[56] James GM. Majority vote classifiers: theory and applications, 1998.

[57] MubarakAli D. Comprehensive Review on Rapid Diagnosis of New Infection COVID-19. Appl Biochem Biotechnol 2022;194:1390–400. https://doi.org/10.1007/s12010-021-03728-0.

[58] Kucirka LM, Lauer SA, Laeyendecker O, Boon D, Lessler J. Variation in False-Negative Rate of Reverse Transcriptase Polymerase Chain Reaction–Based SARS-CoV-2 Tests by Time Since Exposure. Ann Intern Med 2020;173:262–7. https://doi.org/10.7326/M20-1495.

[59] World Health Organisation. COVID-19 Use of chest imaging in COVID-19 a rapid advice guide. 2020.

[60] Benmalek E, Elmhamdi J, Jilbab A. Comparing CT scan and chest X-ray imaging for COVID-19 diagnosis. Biomed Eng Adv 2021;1:100003. https://doi.org/https://doi.org/10.1016/j.bea.2021.100003.

[61] Fang Y, Zhang H, Xie J, Lin M, Ying L, Pang P, et al. Sensitivity of Chest CT for COVID-19: Comparison to RT-PCR. Radiology 2020;296:E115–7. https://doi.org/10.1148/radiol.2020200432.

[62] Li K, Liu X, Yip R, Yankelevitz DF, Henschke CI, Geng Y, et al. Early prediction of severity in coronavirus disease (COVID-19) using quantitative CT imaging. Clin Imaging 2021;78:223–9. https://doi.org/10.1016/j.clinimag.2021.02.003.

[63] Pan F, Ye T, Sun P, Gui S, Liang B, Li L, et al. Time Course of Lung Changes at Chest CT during Recovery from Coronavirus Disease 2019 (COVID-19). Radiology 2020;295:715–21. https://doi.org/10.1148/radiol.2020200370.

[64] Bernheim A, Mei X, Huang M, Yang Y, Fayad ZA, Zhang N, et al. Chest CT Findings in Coronavirus Disease-19 (COVID-19): Relationship to Duration of Infection. Radiology 2020;295:200463. https://doi.org/10.1148/radiol.2020200463.
[65] Kwee TC, Kwee RM. Chest CT in COVID-19: What the Radiologist Needs to Know. Radiographics 2020;40:1848–65. https://doi.org/10.1148/rg.2020200159.
[66] Jacobi A, Chung M, Bernheim A, Eber C. Portable chest X-ray in coronavirus disease-19 (COVID-19): A pictorial review. Clin Imaging 2020;64:35–42. https://doi.org/https://doi.org/10.1016/j.clinimag.2020.04.001.
[67] Swapnarekha H, Behera HS, Nayak J, Naik B. Role of intelligent computing in COVID-19 prognosis: A state-of-the-art review. Chaos, Solitons & Fractals 2020;138:109947. https://doi.org/https://doi.org/10.1016/j.chaos.2020.109947.
[68] Rousan LA, Elobeid E, Karrar M, Khader Y. Chest X-ray findings and temporal lung changes in patients with COVID-19 pneumonia. BMC Pulm Med 2020;20:245. https://doi.org/10.1186/s12890-020-01286-5.
[69] Panwar H, Gupta PK, Siddiqui MK, Morales-Menendez R, Singh V. Application of deep learning for fast detection of COVID-19 in X-rays using nCOVnet. Chaos, Solitons & Fractals 2020;138:109944. https://doi.org/https://doi.org/10.1016/j.chaos.2020.109944.
[70] Toğaçar M, Ergen B, Cömert Z. COVID-19 detection using deep learning models to exploit Social Mimic Optimization and structured chest X-ray images using fuzzy color and stacking approaches. Comput Biol Med 2020;121:103805. https://doi.org/10.1016/j.compbiomed.2020.103805.
[71] Abbas A, Abdelsamea MM, Gaber MM. Classification of COVID-19 in chest X-ray images using DeTraC deep convolutional neural network. Appl Intell 2020. https://doi.org/10.1007/s10489-020-01829-7.
[72] Ucar F, Korkmaz D. COVIDiagnosis-Net: Deep Bayes-SqueezeNet based diagnosis of the coronavirus disease 2019 (COVID-19) from X-ray images. Med Hypotheses 2020;140:109761. https://doi.org/https://doi.org/10.1016/j.mehy.2020.109761.
[73] Ozturk T, Talo M, Yildirim EA, Baloglu UB, Yildirim O, Rajendra Acharya U. Automated detection of COVID-19 cases using deep neural networks with X-ray images. Comput Biol Med 2020;121:103792. https://doi.org/https://doi.org/10.1016/j.compbiomed.2020.103792.
[74] Pereira RM, Bertolini D, Teixeira LO, Silla CN, Costa YMG. COVID-19 identification in chest X-ray images on flat and hierarchical classification scenarios. Comput Methods Programs Biomed 2020;194:105532. https://doi.org/https://doi.org/10.1016/j.cmpb.2020.105532.
[75] Khan AI, Shah JL, Bhat MM. CoroNet: A deep neural network for detection and diagnosis of COVID-19 from chest X-ray images. Comput Methods Programs Biomed 2020;196:105581. https://doi.org/https://doi.org/10.1016/j.cmpb.2020.105581.
[76] Apostolopoulos ID, Aznaouridis SI, Tzani MA. Extracting Possibly Representative COVID-19 Biomarkers from X-ray Images with Deep Learning Approach and Image Data Related to Pulmonary Diseases. J Med Biol Eng 2020;40:462–9. https://doi.org/10.1007/s40846-020-00529-4.
[77] Loey M, Smarandache F, M. Khalifa NE. Within the Lack of Chest COVID-19 X-ray Dataset: A Novel Detection Model Based on GAN and Deep Transfer Learning. Symmetry (Basel) 2020;12:651. https://doi.org/https://doi.org/10.3390/sym12040651.
[78] Apostolopoulos ID, Mpesiana TA. COVID-19: automatic detection from X-ray images utilizing transfer learning with convolutional neural networks. Phys Eng Sci Med 2020;43:635–40. https://doi.org/10.1007/s13246-020-00865-4.
[79] Rahimzadeh M, Attar A. A modified deep convolutional neural network for detecting COVID-19 and pneumonia from chest X-ray images based on the concatenation of Xception and ResNet50V2. Informatics Med Unlocked 2020;19:100360. https://doi.org/https://doi.org/10.1016/j.imu.2020.100360.
[80] Vaid S, Kalantar R, Bhandari M. Deep learning COVID-19 detection bias: accuracy through artificial intelligence. Int Orthop 2020;44:1539–42. https://doi.org/10.1007/s00264-020-04609-7.
[81] Das D, Santosh KC, Pal U. Truncated inception net: COVID-19 outbreak screening using chest X-rays. Phys Eng Sci Med 2020;43:915–25. https://doi.org/10.1007/s13246-020-00888-x.
[82] Oh Y, Park S, Ye JC. Deep Learning COVID-19 Features on CXR Using Limited Training Data Sets. IEEE Trans Med Imaging 2020;39:2688–700. https://doi.org/10.1109/TMI.2020.2993291.
[83] Shibly KH, Dey SK, Islam MT-U, Rahman MM. COVID faster R–CNN: A novel framework to Diagnose Novel Coronavirus Disease (COVID-19) in X-ray images. Informatics Med Unlocked 2020;20:100405. https://doi.org/https://doi.org/10.1016/j.imu.2020.100405.
[84] Yoo SH, Geng H, Chiu TL, Yu SK, Cho DC, Heo J, et al. Deep Learning-Based Decision-Tree

Classifier for COVID-19 Diagnosis From Chest X-ray Imaging. Front Med 2020;7:427. https://doi.org/10.3389/fmed.2020.00427.

[85] Tsiknakis N, Trivizakis E, Vassalou EE, Papadakis GZ, Spandidos DA, Tsatsakis A, et al. Interpretable artificial intelligence framework for COVID-19 screening on chest X-rays. Exp Ther Med 2020;20:727–35. https://doi.org/10.3892/etm.2020.8797.

[86] Nour M, Cömert Z, Polat K. A Novel Medical Diagnosis model for COVID-19 infection detection based on Deep Features and Bayesian Optimization. Appl Soft Comput 2020:106580. https://doi.org/https://doi.org/10.1016/j.asoc.2020.106580.

[87] Zebin T, Rezvy S. COVID-19 detection and disease progression visualization: Deep learning on chest X-rays for classification and coarse localization. Appl Intell 2021;51:1010–21. https://doi.org/10.1007/s10489-020-01867-1.

[88] Pandit MK, Banday SA, Naaz R, Chishti MA. Automatic detection of COVID-19 from chest radiographs using deep learning. Radiography 2021;27:483–9. https://doi.org/https://doi.org/10.1016/j.radi.2020.10.018.

[89] Singh RK, Pandey R, Babu RN. COVIDScreen: explainable deep learning framework for differential diagnosis of COVID-19 using chest X-rays. Neural Comput Appl 2021. https://doi.org/10.1007/s00521-020-05636-6.

[90] Jain G, Mittal D, Thakur D, Mittal MK. A deep learning approach to detect COVID-19 coronavirus with X-ray images. Biocybern Biomed Eng 2020;40:1391–405. https://doi.org/https://doi.org/10.1016/j.bbe.2020.08.008.

[91] Ouchicha C, Ammor O, Meknassi M. CVDNet: A novel deep learning architecture for detection of coronavirus (COVID-19) from chest X-ray images. Chaos, Solitons & Fractals 2020;140:110245. https://doi.org/https://doi.org/10.1016/j.chaos.2020.110245.

[92] Murugan R, Goel T. E-DiCoNet: Extreme learning machine based classifier for diagnosis of COVID-19 using deep convolutional network. J Ambient Intell Humaniz Comput 2021;12:8887–98. https://doi.org/10.1007/s12652-020-02688-3.

[93] Jin W, Dong S, Dong C, Ye X. Hybrid ensemble model for differential diagnosis between COVID-19 and common viral pneumonia by chest X-ray radiograph. Comput Biol Med 2021;131:104252. https://doi.org/10.1016/j.compbiomed.2021.104252.

[94] Shankar K, Mohanty SN, Yadav K, Gopalakrishnan T, Elmisery AM. Automated COVID-19 diagnosis and classification using convolutional neural network with fusion based feature extraction model. Cogn Neurodyn 2021. https://doi.org/10.1007/s11571-021-09712-y.

[95] Azouji N, Sami A, Taheri M, Müller H. A large margin piecewise linear classifier with fusion of deep features in the diagnosis of COVID-19. Comput Biol Med 2021;139:104927. https://doi.org/https://doi.org/10.1016/j.compbiomed.2021.104927.

[96] Butt C, Gill J, Chun D, Babu BA. RETRACTED ARTICLE: Deep learning system to screen coronavirus disease 2019 pneumonia. Appl Intell 2020. https://doi.org/10.1007/s10489-020-01714-3.

[97] Jaiswal A, Gianchandani N, Singh D, Kumar V, Kaur M. Classification of the COVID-19 infected patients using DenseNet201 based deep transfer learning. J Biomol Struct Dyn 2020;0:1–8. https://doi.org/10.1080/07391102.2020.1788642.

[98] Wu X, Hui H, Niu M, Li L, Wang L, He B, et al. Deep learning-based multi-view fusion model for screening 2019 novel coronavirus pneumonia: A multicentre study. Eur J Radiol 2020;128:109041. https://doi.org/https://doi.org/10.1016/j.ejrad.2020.109041.

[99] Harmon SA, Sanford TH, Xu S, Turkbey EB, Roth H, Xu Z, et al. Artificial intelligence for the detection of COVID-19 pneumonia on chest CT using multinational datasets. Nat Commun 2020;11:4080. https://doi.org/10.1038/s41467-020-17971-2.

[100] Ardakani AA, Kanafi AR, Acharya UR, Khadem N, Mohammadi A. Application of deep learning technique to manage COVID-19 in routine clinical practice using CT images: Results of 10 convolutional neural networks. Comput Biol Med 2020;121:103795. https://doi.org/https://doi.org/10.1016/j.compbiomed.2020.103795.

[101] Ouyang X, Huo J, Xia L, Shan F, Liu J, Mo Z, et al. Dual-Sampling Attention Network for Diagnosis of COVID-19 From Community Acquired Pneumonia. IEEE Trans Med Imaging 2020;39:2595–605. https://doi.org/10.1109/TMI.2020.2995508.

[102] Yang S, Jiang L, Cao Z, Wang L, Cao J, Feng R, et al. Deep learning for detecting corona virus disease 2019 (COVID-19) on high-resolution computed tomography: a pilot study. Ann Transl Med 2020;8:450. https://doi.org/10.21037/atm.2020.03.132.

[103] Han Z, Wei B, Hong Y, Li T, Cong J, Zhu X, et al. Accurate Screening of COVID-19 Using Attention-Based Deep 3D Multiple Instance Learning. IEEE Trans Med Imaging 2020;39:2584–94. https://doi.org/10.1109/TMI.2020.2996256.

[104] Hasan AM, AL-Jawad MM, Jalab HA, Shaiba H, Ibrahim RW, AL-Shamasneh AR. Classification of COVID-19 Coronavirus, Pneumonia and Healthy Lungs in CT Scans Using Q-Deformed Entropy and Deep Learning Features. Entropy 2020;22:517. https://doi.org/https://doi.org/10.3390/e22050517.
[105] Pu J, Leader J, Bandos A, Shi J, Du P, Yu J, et al. Any unique image biomarkers associated with COVID-19? Eur Radiol 2020;30:6221–7. https://doi.org/10.1007/s00330-020-06956-w.
[106] Pathak Y, Shukla PK, Tiwari A, Stalin S, Singh S, Shukla PK. Deep Transfer Learning Based Classification Model for COVID-19 Disease. IRBM 2020. https://doi.org/https://doi.org/10.1016/j.irbm.2020.05.003.
[107] Singh D, Kumar V, Vaishali, Kaur M. Classification of COVID-19 patients from chest CT images using multi-objective differential evolution–based convolutional neural networks. Eur J Clin Microbiol Infect Dis 2020;39:1379–89. https://doi.org/10.1007/s10096-020-03901-z.
[108] Song J, Wang H, Liu Y, Wu W, Dai G, Wu Z, et al. End-to-end automatic differentiation of the coronavirus disease 2019 (COVID-19) from viral pneumonia based on chest CT. Eur J Nucl Med Mol Imaging 2020;47:2516–24. https://doi.org/10.1007/s00259-020-04929-1.
[109] Xie W, Jacobs C, Charbonnier J-P, van Ginneken B. Relational Modeling for Robust and Efficient Pulmonary Lobe Segmentation in CT Scans. IEEE Trans Med Imaging 2020;39:2664–75. https://doi.org/10.1109/TMI.2020.2995108.
[110] Hu S, Gao Y, Niu Z, Jiang Y, Li L, Xiao X, et al. Weakly Supervised Deep Learning for COVID-19 Infection Detection and Classification From CT Images. IEEE Access 2020;8:118869–83. https://doi.org/10.1109/ACCESS.2020.3005510.
[111] Wang S, Zha Y, Li W, Wu Q, Li X, Niu M, et al. A Fully Automatic Deep Learning System for COVID-19 Diagnostic and Prognostic Analysis. Eur Respir J 2020. https://doi.org/10.1183/13993003.00775-2020.
[112] Konar D, Panigrahi BK, Bhattacharyya S, Dey N. Auto-diagnosis of COVID-19 using Lung CT Images with Semi-supervised Shallow Learning Network 2020. https://doi.org/10.21203/rs.3.rs-34596/v1.
[113] Ko H, Chung H, Kang WS, Kim KW, Shin Y, Kang SJ, et al. COVID-19 Pneumonia Diagnosis Using a Simple 2D Deep Learning Framework With a Single Chest CT Image: Model Development and Validation. J Med Internet Res 2020;22:e19569. https://doi.org/10.2196/19569.
[114] Wang S, Kang B, Ma J, Zeng X, Xiao M, Guo J, et al. A deep learning algorithm using CT images to screen for Corona virus disease (COVID-19). Eur Radiol 2021. https://doi.org/10.1007/s00330-021-07715-1.
[115] Chen J, Wu L, Zhang J, Zhang L, Gong D, Zhao Y, et al. Deep learning-based model for detecting 2019 novel coronavirus pneumonia on high-resolution computed tomography. Sci Rep 2020;10:19196. https://doi.org/10.1038/s41598-020-76282-0.
[116] Song Y, Zheng S, Li L, Zhang X, Zhang X, Huang Z, et al. Deep learning Enables Accurate Diagnosis of Novel Coronavirus (COVID-19) with CT images. IEEE/ACM Trans Comput Biol Bioinforma 2021:1. https://doi.org/10.1109/TCBB.2021.3065361.
[117] Serte S, Demirel H. Deep learning for diagnosis of COVID-19 using 3D CT scans. Comput Biol Med 2021;132:104306. https://doi.org/10.1016/j.compbiomed.2021.104306.
[118] Li Q, Ning J, Yuan J, Xiao L. A depthwise separable dense convolutional network with convolution block attention module for COVID-19 diagnosis on CT scans. Comput Biol Med 2021;137:104837. https://doi.org/10.1016/j.compbiomed.2021.104837.
[119] Canayaz M. C+EffxNet: A novel hybrid approach for COVID-19 diagnosis on CT images based on CBAM and EfficientNet. Chaos, Solitons & Fractals 2021;151:111310. https://doi.org/10.1016/j.chaos.2021.111310.
[120] Chen X, Yao L, Zhou T, Dong J, Zhang Y. Momentum contrastive learning for few-shot COVID-19 diagnosis from chest CT images. Pattern Recognit 2021;113:107826. https://doi.org/https://doi.org/10.1016/j.patcog.2021.107826.
[121] Sedik A, Hammad M, Abd El-Samie FE, Gupta BB, Abd El-Latif AA. Efficient deep learning approach for augmented detection of Coronavirus disease. Neural Comput Appl 2021. https://doi.org/10.1007/s00521-020-05410-8.
[122] Goswami T. Impact of Deep Learning in Image Processing and Computer Vision BT - Microelectronics, Electromagnetics and Telecommunications. In: Anguera J, Satapathy SC, Bhateja V, Sunitha KVN, editors., Singapore: Springer Singapore; 2018, p. 475–85.
[123] Anwar SM, Majid M, Qayyum A, Awais M, Alnowami M, Khan MK. Medical Image Analysis using Convolutional Neural Networks: A Review. J Med Syst 2018;42:226. https://doi.org/10.1007/s10916-018-1088-1.

[124] O'Mahony N, Campbell S, Carvalho A, Harapanahalli S, Hernandez GV, Krpalkova L, et al. Deep Learning vs. Traditional Computer Vision. In: Arai K, Kapoor S, editors. Adv. Comput. Vis., Cham: Springer International Publishing; 2020, p. 128–44.
[125] Liu X, Gao K, Liu B, Pan C, Liang K, Yan L, et al. Advances in Deep Learning-Based Medical Image Analysis. Heal Data Sci 2021;2021:8786793. https://doi.org/10.34133/2021/8786793.
[126] Sharma P, Bhatt DP. Importance of Deep Learning Models in the Medical Imaging Field. Approaches Appl. Deep Learn. Virtual Med. Care, 2022, p. 1–23. https://doi.org/10.4018/978-1-7998-8929-8.ch001.
[127] Gaur L, Bhatia U, Jhanjhi NZ, Muhammad G, Masud M. Medical image-based detection of COVID-19 using Deep Convolution Neural Networks. Multimed Syst 2021. https://doi.org/10.1007/s00530-021-00794-6.
[128] Sethi R, Mehrotra M, Sethi D. Deep Learning based Diagnosis Recommendation for COVID-19 using Chest X-rays Images. 2020 Second Int. Conf. Inven. Res. Comput. Appl., 2020, p. 1–4. https://doi.org/10.1109/ICIRCA48905.2020.9183278.
[129] Khan A, Sohail A, Zahoora U, Qureshi AS. A survey of the recent architectures of deep convolutional neural networks. Artif Intell Rev 2020;53:5455–516. https://doi.org/10.1007/s10462-020-09825-6.
[130] Simonyan K, Zisserman A. Very deep convolutional networks for large-scale image recognition. ArXiv Prepr ArXiv14091556 2014.
[131] Nguyen H-G, Pica A, Hrbacek J, Weber DC, La Rosa F, Schalenbourg A, et al. A novel segmentation framework for uveal melanoma in magnetic resonance imaging based on class activation maps. Int. Conf. Med. Imaging with Deep Learn., PMLR; 2019, p. 370–9.
[132] Wang T, Lei Y, Fu Y, Wynne JF, Curran WJ, Liu T, et al. A review on medical imaging synthesis using deep learning and its clinical applications. J Appl Clin Med Phys 2021;22:11–36. https://doi.org/10.1002/acm2.13121.
[133] Acar E, Şahin E, Yılmaz İ. Improving effectiveness of different deep learning-based models for detecting COVID-19 from computed tomography (CT) images. Neural Comput Appl 2021;33:17589–609. https://doi.org/10.1007/s00521-021-06344-5.
[134] Dhont J, Wolfs C, Verhaegen F. Automatic coronavirus disease 2019 diagnosis based on chest radiography and deep learning {\textendash} Success story or dataset bias? Med Phys 2022;49:978–87. https://doi.org/10.1002/mp.15419.
[135] Zargari Khuzani A, Heidari M, Shariati SA. COVID-Classifier: an automated machine learning model to assist in the diagnosis of COVID-19 infection in chest X-ray images. Sci Rep 2021;11:9887. https://doi.org/10.1038/s41598-021-88807-2.
[136] Aljondi R, Alghamdi S. Diagnostic Value of Imaging Modalities for COVID-19: Scoping Review. J Med Internet Res 2020;22:e19673. https://doi.org/10.2196/19673.
[137] Wu Y-H, Gao S-H, Mei J, Xu J, Fan D-P, Zhang R-G, et al. JCS: An Explainable COVID-19 Diagnosis System by Joint Classification and Segmentation. IEEE Trans Image Process 2021;30:3113–26. https://doi.org/10.1109/TIP.2021.3058783.
[138] Axiaq A, Almohtadi A, Massias SA, Ngemoh D, Harky A. The role of computed tomography scan in the diagnosis of COVID-19 pneumonia. Curr Opin Pulm Med 2021;27:163–8. https://doi.org/10.1097/MCP.0000000000000765.
[139] El-Rashidy N, Abdelrazik S, Abuhmed T, Amer E, Ali F, Hu J-W, et al. Comprehensive Survey of Using Machine Learning in the COVID-19 Pandemic. Diagnostics 2021;11. https://doi.org/10.3390/diagnostics11071155.
[140] Tung-Chen Y, Martí de Gracia M, Díez-Tascón A, Alonso-González R, Agudo-Fernández S, Parra-Gordo ML, et al. Correlation between Chest Computed Tomography and Lung Ultrasonography in Patients with Coronavirus Disease 2019 (COVID-19). Ultrasound Med Biol 2020;46:2918–26. https://doi.org/https://doi.org/10.1016/j.ultrasmedbio.2020.07.003.
[141] Rehouma R, Buchert M, Chen Y-PP. Machine learning for medical imaging-based COVID-19 detection and diagnosis. Int J Intell Syst 2021;36:5085–115. https://doi.org/https://doi.org/10.1002/int.22504.
[142] Khalili N, Haseli S, Iranpour P. Lung Ultrasound in COVID-19 Pneumonia: Prospects and Limitations. Acad Radiol 2020;27:1044–5. https://doi.org/10.1016/j.acra.2020.04.032.
[143] Vasilev YA, Sergunova KA, Bazhin A V, Masri AG, Vasileva YN, Semenov DS, et al. Chest MRI of patients with COVID-19. Magn Reson Imaging 2021;79:13–9. https://doi.org/https://doi.org/10.1016/j.mri.2021.03.005.
[144] Lu G, Fei B. Medical hyperspectral imaging: a review. J Biomed Opt 2014;19:1–24. https://doi.org/10.1117/1.JBO.19.1.010901.
[145] Alafeef M, Moitra P, Dighe K, Pan D. Hyperspectral Mapping for the Detection of SARS-CoV-2

Using Nanomolecular Probes with Yoctomole Sensitivity. ACS Nano 2021;15:13742–58. https://doi.org/10.1021/acsnano.1c05226.

[146] Brahim Belhaouari D, Fontanini A, Baudoin J-P, Haddad G, Le Bideau M, Bou Khalil JY, et al. The Strengths of Scanning Electron Microscopy in Deciphering SARS-CoV-2 Infectious Cycle. Front Microbiol 2020;11:2014. https://doi.org/10.3389/fmicb.2020.02014.

[147] Inkson BJ. 2 - Scanning electron microscopy (SEM) and transmission electron microscopy (TEM) for materials characterization. In: Hübschen G, Altpeter I, Tschuncky R, Herrmann H-G, editors. Mater. Charact. Using Nondestruct. Eval. Methods, Woodhead Publishing; 2016, p. 17–43. https://doi.org/https://doi.org/10.1016/B978-0-08-100040-3.00002-X.

[148] Han T, Liu C, Wu R, Jiang D. Deep transfer learning with limited data for machinery fault diagnosis. Appl Soft Comput 2021;103:107150. https://doi.org/10.1016/j.asoc.2021.107150.

[149] Amyar A, Modzelewski R, Li H, Ruan S. Multi-task deep learning based CT imaging analysis for COVID-19 pneumonia: Classification and segmentation. Comput Biol Med 2020;126:104037. https://doi.org/https://doi.org/10.1016/j.compbiomed.2020.104037.

[150] Jin S, Wang B, Xu H, Luo C, Wei L, Zhao W, et al. AI-assisted CT imaging analysis for COVID-19 screening: Building and deploying a medical AI system in four weeks. MedRxiv 2020:2020.03.19.20039354. https://doi.org/10.1101/2020.03.19.20039354.

[151] Gaál G, Maga B, Lukács A. Attention U-Net Based Adversarial Architectures for Chest X-ray Lung Segmentation. ArXiv E-Prints 2020:arXiv:2003.10304.

[152] Oktay O, Schlemper J, Folgoc L Le, Lee MCH, Heinrich MP, Misawa K, et al. Attention U-Net: Learning Where to Look for the Pancreas. CoRR 2018;abs/1804.0.

[153] Dai W-C, Zhang H-W, Yu J, Xu H-J, Chen H, Luo S-P, et al. CT Imaging and Differential Diagnosis of COVID-19. Can Assoc Radiol J = J l'Association Can Des Radiol 2020;71:195–200. https://doi.org/10.1177/0846537120913033.

[154] Duzgun SA, Durhan G, Demirkazik FB, Akpinar MG, Ariyurek OM. COVID-19 pneumonia: the great radiological mimicker. Insights Imaging 2020;11:118. https://doi.org/10.1186/s13244-020-00933-z.

[155] Li Y, Wang H, Wang F, Du H, Liu X, Chen P, et al. Comparison of hospitalized patients with pneumonia caused by COVID-19 and influenza A in children under 5 years. Int J Infect Dis 2020;98:80–3. https://doi.org/10.1016/j.ijid.2020.06.026.

[156] Hani C, Trieu NH, Saab I, Dangeard S, Bennani S, Chassagnon G, et al. COVID-19 pneumonia: A review of typical CT findings and differential diagnosis. Diagn Interv Imaging 2020;101:263–8. https://doi.org/10.1016/j.diii.2020.03.014.

[157] Zhao D, Yao F, Wang L, Zheng L, Gao Y, Ye J, et al. A Comparative Study on the Clinical Features of Coronavirus 2019 (COVID-19) Pneumonia With Other Pneumonias. Clin Infect Dis 2020;71:756–61. https://doi.org/10.1093/cid/ciaa247.

[158] Bejani MM, Ghatee M. A systematic review on overfitting control in shallow and deep neural networks. Artif Intell Rev 2021. https://doi.org/10.1007/s10462-021-09975-1.

[159] Polikar R. Ensemble Learning BT - Ensemble Machine Learning: Methods and Applications. In: Zhang C, Ma Y, editors., Boston, MA: Springer US; 2012, p. 1–34. https://doi.org/10.1007/978-1-4419-9326-7_1.

[160] Chen Z, Zhang Y, Simsek M, Kantarci B. Deep Belief Network-based Fake Task Mitigation for Mobile Crowdsensing under Data Scarcity. ICC 2020 - 2020 IEEE Int. Conf. Commun., 2020, p. 1–7. https://doi.org/10.1109/ICC40277.2020.9148817.

[161] Huang P, Liu T, Huang L, Liu H, Lei M, Xu W, et al. Use of Chest CT in Combination with Negative RT-PCR Assay for the 2019 Novel Coronavirus but High Clinical Suspicion. Radiology 2020;295:22–3. https://doi.org/10.1148/radiol.2020200330.